Jpn J Ophthalmol
Vol 52: 99–107, 2008

after treatment, resolution of fluid and hemorrhage were noted, with a best-corrected visual acuity letter score of 64 ($20/50^{-1}$). After enrollment in the JAT Extension, she received further treatment with verteporfin therapy at month 24, and best-corrected visual acuity letter score at this visit was 71 ($20/40^{+1}$). Visual acuity remained stable to the final follow-up at month 33, when best-corrected visual acuity letter score was 70 (20/40).

Patient 2 (Fig. 5) was a 63-year-old man. At baseline, his best-corrected visual acuity letter score was 61 ($20/63^{+1}$) in his right eye, associated with subretinal fluid, hemorrhage, and drusen, as well as multifocal areas of retinal pigment epithelial abnormalities. The patient received verteporfin therapy at baseline, month 3, and month 9. One year after initiation of verteporfin therapy, he had a letter score of 71 ($20/40^{+1}$); subretinal fluid and hemorrhage had resolved, with staining of fibrovascular tissue and retinal pigment epithelial abnormalities. The patient enrolled in the extension and received further treatment at month 15. At month 18, he discontinued because of an intercurrent illness, and best-corrected visual acuity letter score was 74 ($20/32^{-1}$) at this visit.

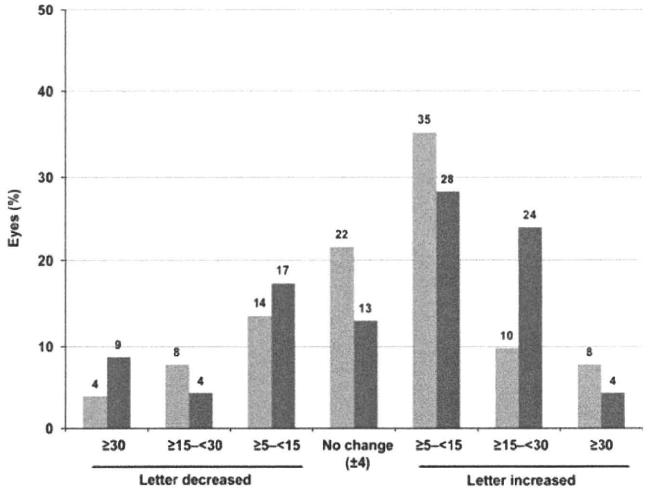

Figure 3. Visual acuity change from baseline at month 12 to month 24 in the JAT Extension. *Light gray bars*, month 12 ($n = 51$); *dark gray bars*, month 24 ($n = 46$).

Discussion

The objective of this extension study was to assess longer term safety of verteporfin therapy in Japanese AMD patients. The incidence of adverse events in the JAT Extension was comparable to the incidence in both the first year of JAT and the 24-month findings in the TAP Investigation.[5,14] Overall, the safety profile of the JAT Extension appears similar to that of the first 12 months of the study. However, fewer adverse events occurred in extension patients during the extension phase (118) than during the first 12 months (180) of the trial. Of the events that occurred during the extension, 12% were considered to be possibly or probably related to the study drug, compared with 26% during the first 12 months. The ocular safety profile during the extension was also similar to that reported during the first 12 months. Eight patients had a visual disturbance in the study eye during the extension, compared with nine patients during the first 12 months. Most of these visual disturbances were vision decreases, which occurred in seven patients during the first 12 months and a further seven during the extension (14 patients in total). There was no report of acute severe visual acuity decrease during the JAT Extension. Acute severe visual acuity decrease had been reported previously in 0.7% of patients in the TAP Investigation and 4.4% of patients in the Verteporfin in Photodynamic Therapy trial.[15] No additional safety concerns were identified during the second year of follow-up, and the data confirm the safety profile previously reported in the TAP Investigation[5,13] and TAP Extension.[16–18]

The treatment course number of each adverse event was recorded to investigate any cumulative effects of verteporfin therapy. No consistent pattern was observed for the incidence of adverse events for any particular body system or for any particular adverse event in relation to the number of treatment courses. No cumulative toxic effect of verteporfin therapy was therefore observed throughout 2 years of treatment.

A comparison of the visual acuity outcomes at month 12 for the 64 patients enrolled in JAT and at month 24 for the 46 JAT Extension patients who completed this visit is given in Table 3. The overall beneficial effects on visual acuity outcomes reported previously[14] were sustained through 24 months of follow-up. At month 12, 73% of 64 patients in JAT had stable (±4 letter change) or improved visual

Table 3. Comparison of 12- and 24-month visual acuity outcomes in JAT

Vision outcomes	JAT month 12 % ($n = 64$)[a]	JAT Extension month 24 % ($n = 46$)
≥30-letter increase (≥6 lines)	6	4
≥15- to <30-letter increase (≥3 to <6 lines)	14	24
≥5- to <15-letter increase (≥1 to <3 lines)	33	28
Stable (±4 letters)	20	13
≥5- to <15-letter decrease (≥1 to <3 lines)	13	17
≥15- to <30-letter decrease (≥1 to <3 lines)	11	4
≥30-letter decrease (≥6 lines)	3	9

[a]JAT 12-month results use the method of the last observation carried forward.

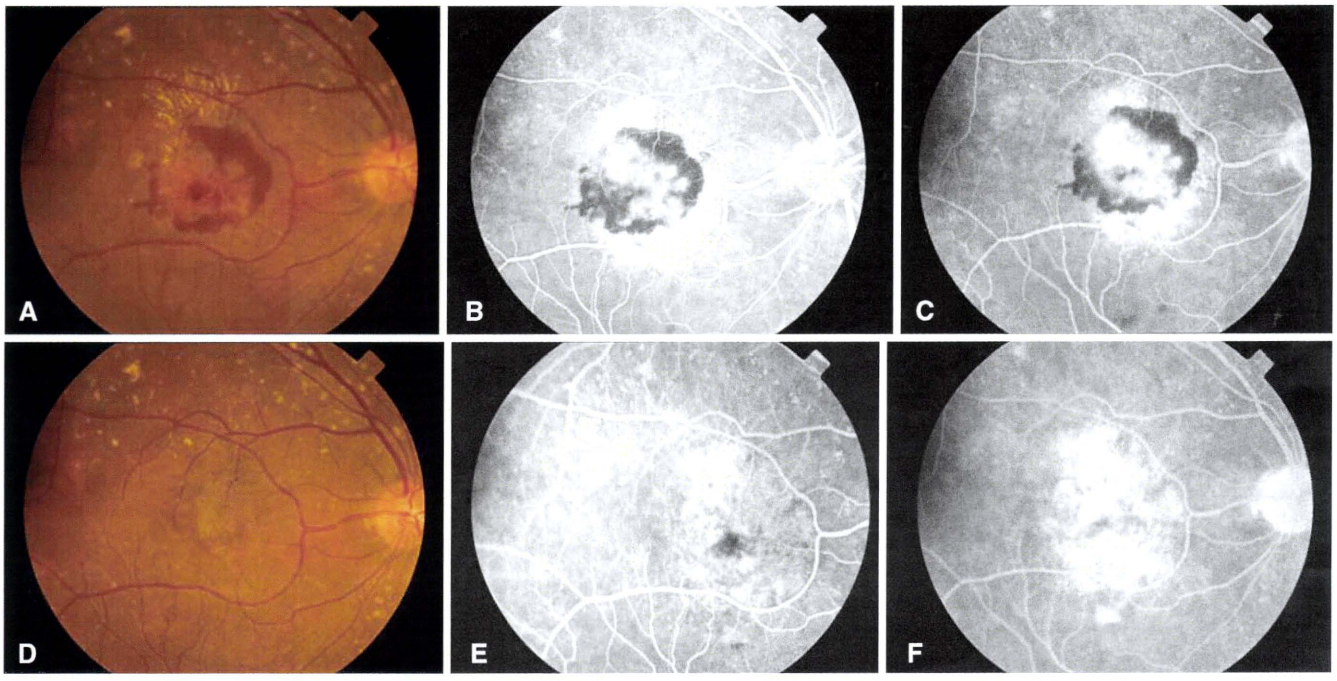

Figure 4A–F. At baseline, the initial visual acuity letter score was 52 (approximate Snellen equivalent, $20/100^{+2}$). **A** Color fundus photograph shows hemorrhage surrounding choroidal neovascular lesion with additional lipid superior to the lesion and large drusen, seen predominantly in the superior portion of the posterior pole. **B** Early-phase fluorescein angiogram shows hyperfluorescence surrounded by hypofluorescence from blood surrounded by stippled fluorescence. **C** Late-phase frame shows leakage from the central hyperfluorescence, persistent hypofluorescence from the blood, and staining of the retinal pigment epithelial abnormalities. At the month 12 visit, the visual acuity letter score was 64 ($20/50^{-1}$). **D** Color fundus photograph shows resolution of the hemorrhage with the early-phase fluorescein angiogram (**E**) showing staining of the retinal pigment epithelial abnormalities with persistent staining but no obvious leakage from these pigment epithelial abnormalities in the late-phase frame (**F**).

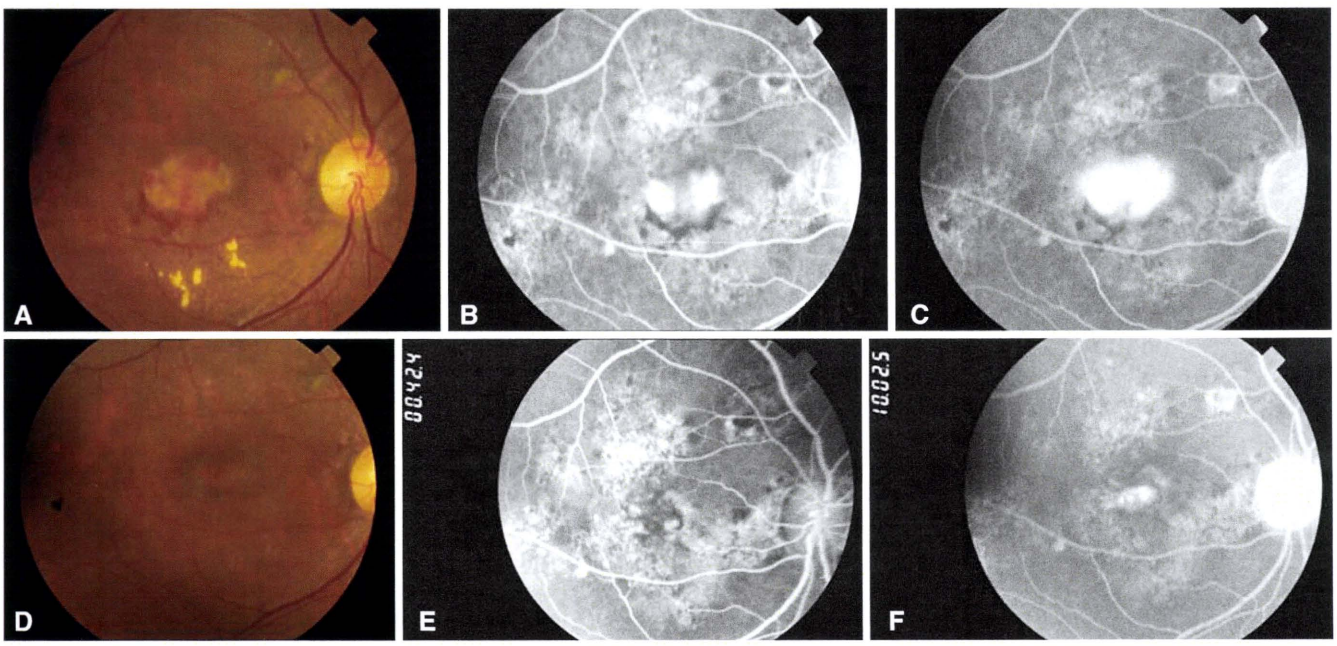

Figure 5A–F. At baseline, initial visual acuity letter score was 61 (approximate Snellen equivalent, $20/63^{+1}$). **A** Color fundus photograph shows fibrovascular tissue with hemorrhage along the inferior aspect of the tissue with additional lipid. **B** Fluorescein angiography shows hyperfluorescence in the central macula with hypofluorescence corresponding to hemorrhage along the inferior aspect of the hyperfluorescence and additional multifocal areas of pigment epithelial abnormalities. **C** Late-phase frame shows leakage from the central hyperfluorescence consistent with choroidal neovascularization and staining of the multifocal areas of the pigment epithelial abnormality throughout the posterior pole. At month 12, the visual acuity letter score was 71 ($20/40^{+1}$). **D** Color fundus photograph shows resolution of the subretinal fluid and hemorrhage. Fluorescein angiography shows staining of pigment epithelial abnormalities in the early-phase frame (**E**) with persistent staining but no leakage of fibrovascular tissue within central macula in the late-phase frame (**F**), as well as less fluorescent staining of multifocal pigment epithelial abnormalities throughout the posterior pole.

Jpn J Ophthalmol
Vol 52: 99–107, 2008

acuity;[14] by month 24. Thirty-two (70%) of the 46 patients still participating in the JAT Extension had stable or improved visual acuity.

By month 24 in the TAP Investigation, 121 (30%) of 402 verteporfin-treated patients had stable or improved visual acuity.[5] The TAP Investigation used the method of last observation carried forward, which was not used in the JAT Extension; therefore, the 24-month results cannot be compared directly between these studies. As noted in the JAT 12-month report,[14] although the inclusion/exclusion criteria were the same, JAT and the TAP investigations are not directly comparable because there were some differences in patient baseline characteristics between the two studies. These differences included a higher percentage of men, a slightly lower mean age, a smaller lesion size, and fewer predominantly classic lesions in the JAT than in the TAP investigation. However, retrospective analyses suggested that the differences in baseline characteristics between the two studies could not fully explain the improved visual acuity outcomes in JAT patients.[14] These differences in outcomes are consistent with previous studies comparing outcomes between predominantly Caucasian and Asian populations.[16]

The average number of treatments administered during the second 12-month period (0.9) was lower than the average number during the first 12 months (3.0) as the need for treatment decreased with each month of follow-up. These treatment averages are lower than the average number of treatments required by the primarily Caucasian patients in the TAP Investigation, where the average number of treatments was 3.4 in the first year and 2.2 in the second year.[5] The significance of this finding is not known.

Overall, these results show that verteporfin therapy is safe, and had beneficial effects in terms of stabilizing or improving visual acuity through to the end of the trial (up to 33 months), which were similar results to those observed in the TAP investigation[5,13] and the TAP Extension.[17–19]

Conclusions

The results from the JAT Extension provide further compelling evidence for the safety of verteporfin therapy in Japanese patients with subfoveal CNV secondary to AMD. The effects on visual acuity and fluorescein angiography seemed similar to those observed in the TAP investigation, and therefore supported the long-term use of verteporfin therapy in Japanese patients with subfoveal CNV secondary to AMD.

Acknowledgments. The authors acknowledge the writing and editorial assistance of Rebecca Ireland, BA (Hons) Cantab and Elizabeth Poole PhD (Chameleon Communications International, London, UK), sponsored by Novartis Pharma AG, in the preparation of this manuscript. This study was supported financially by Novartis Pharma AG, Basel, Switzerland, and QLT Inc, Vancouver, British Columbia, Canada.

References

1. Buch H, Vinding T, La Cour M, et al. Prevalence and causes of visual impairment and blindness among 9980 Scandinavian adults: the Copenhagen City Eye Study. Ophthalmology 2004;111:53–61.
2. Congdon N, O'Colmain B, Klaver CC, et al. Causes and prevalence of visual impairment among adults in the United States. Arch Ophthalmol 2004;122:477–485.
3. Dimitrov PN, Mukesh BN, McCarty CA, Taylor HR. Five-year incidence of bilateral cause-specific visual impairment in the Melbourne Visual Impairment Project. Invest Ophthalmol Vis Sci 2003;44:5075–5081.
4. Foran S, Wang JJ, Mitchell P. Causes of visual impairment in two older population cross-sections: the Blue Mountains Eye Study. Ophthalmic Epidemiol 2003;10:215–225.
5. Treatment of Age-Related Macular Degeneration with Photodynamic Therapy (TAP) Study Group. Photodynamic therapy of subfoveal choroidal neovascularization in age-related macular degeneration with verteporfin: two-year results of 2 randomized clinical trials—TAP Report 2. Arch Ophthalmol 2001;119: 198–207.
6. Verteporfin In Photodynamic Therapy (VIP) Study Group. Verteporfin therapy of subfoveal choroidal neovascularization in age-related macular degeneration: two-year results of a randomized clinical trial including lesions with occult with no classic choroidal neovascularization—Verteporfin In Photodynamic Therapy Report 2. Am J Ophthalmol 2001;131:541–560.
7. Visudyne In Minimally Classic CNV (VIM) Study Group. Verteporfin therapy of subfoveal minimally classic choroidal neovascularization in age-related macular degeneration: 2-year results of a randomized clinical trial. Arch Ophthalmol 2005;123:448–457.
8. Verteporfin Roundtable Participants. Guidelines for using verteporfin (Visudyne) in photodynamic therapy for choroidal neovascularization due to age-related macular degeneration and other causes: update. Retina 2005;25:119–134.
9. Lim JI, Kwok A, Wilson DK. Symptomatic age-related macular degeneration in Asian patients. Retina 1998;18:435–438.
10. Pieramici DJ, Bressler NM, Bressler SB, Schachat AP. Choroidal neovascularization in black patients. Arch Ophthalmol 1994;112: 1043–1046.
11. Uyama M, Takahashi K, Ida N, et al. The second eye of Japanese patients with unilateral exudative age related macular degeneration. Br J Ophthalmol 2000;84:1018–1023.
12. Matsui M. Macular diseases in the elderly person (in Japanese with English abstract). Nippon Ganka Gakkai Zasshi (J Jpn Ophthalmol Soc) 1989;93:883–907.
13. Treatment of Age-Related Macular Degeneration with Photodynamic Therapy (TAP) Study Group. Photodynamic therapy of subfoveal choroidal neovascularization in age-related macular degeneration with verteporfin: one-year results of 2 randomized clinical trials—TAP Report 1. Arch Ophthalmol 1999;117: 1329–1345.
14. Japanese Age-Related Macular Degeneration Trial (JAT) Study Group. Japanese age-related macular degeneration trial: 1-year results of photodynamic therapy with verteporfin in Japanese patients with subfoveal choroidal neovascularization secondary to age-related macular degeneration. Am J Ophthalmol 2003;136: 1049–1061.
15. Treatment of Age-Related Macular Degeneration with Photodynamic Therapy (TAP) and Verteporfin In Photodynamic Therapy (VIP) Study Groups. Acute severe visual acuity decrease after photodynamic therapy with verteporfin: case reports from randomized clinical trials—TAP and VIP Report No. 3. Am J Ophthalmol 2004;137:683–696.
16. Chan WM, Lai TY, Tano Y, Liu DT, Li KK, Lam DS. Photodynamic therapy in macular diseases of Asian populations: when East meets West. Jpn J Ophthalmol 2006;50:161–169.
17. Treatment of Age-Related Macular Degeneration with Photodynamic Therapy (TAP) Study Group. Verteporfin therapy for subfoveal choroidal neovascularization in age-related macular

degeneration: three-year results of an open-label extension of 2 randomized clinical trials—TAP Report No. 5. Arch Ophthalmol 2002;120:1307–1314.
18. Treatment of Age-Related Macular Degeneration with Photodynamic Therapy (TAP) Study Group. Verteporfin therapy for subfoveal choroidal neovascularization in age-related macular degeneration: four-year results of an open-label extension of 2 randomized clinical trials: TAP Report No. 7. Arch Ophthalmol 2005;123:1283–1285.
19. Treatment of Age-Related Macular Degeneration with Photodynamic Therapy (TAP) Study Group. Verteporfin therapy of subfoveal choroidal neovascularization in age-related macular degeneration: 5-year results of 2 randomized clinical trials with an open-label extension—TAP Report No. 8. Graefes Arch Clin Exp Ophthalmol 2006;244:1132–1142.

Writing Committee for JAT Extension Report

The following members of the JAT Study Group take authorship responsibility for the JAT Extension Report: Yasuo Tano, (Writing Committee Chair); Neil M. Bressler, Tatsuro Ishibashi, Masahito Ohji, Fumio Shiraga, Kanji Takahashi, Annemarie Weisberger,* and Mitsuko Yuzawa. *Employee of Novartis, which sponsored the trial.

Financial Disclosures

The Johns Hopkins University, but not Dr. N.M. Bressler, is paid for consulting services provided by Dr. N.M. Bressler to Novartis Pharma AG and QLT Inc. The terms of this institutional consulting arrangement are being managed by the Johns Hopkins University in accordance with its conflict of interest policies. The following authors have indicated that they are being or have been paid as consultants to QLT Inc. or Novartis Pharma AG or both (which may also include travel expenses at congresses or participation in a speakers' bureau or advisory board meeting): Tatsuro Ishibashi, Masahito Ohji, Yasuo Tano, Mitsuko Yuzawa. The following authors have indicated that they have received grants from the Japanese Government: Tatsuro Ishibashi, Masahito Ohji, Mitsuko Yuzawa. The following author has indicated that he has received a research grant from the Japanese Ministry of Health, Labour and Welfare: Yasuo Tano.

Intraocular Pressure Elevation after Injection of Triamcinolone Acetonide: A Multicenter Retrospective Case-Control Study

MASARU INATANI, KEIICHIRO IWAO, TAKAHIRO KAWAJI, YOSHIO HIRANO, YUICHIRO OGURA, KAZUYUKI HIROOKA, FUMIO SHIRAGA, YORIKO NAKANISHI, HIROYUKI YAMAMOTO, AKIRA NEGI, YUKA SHIMONAGANO, TAIJI SAKAMOTO, CHIEKO SHIMA, MIYO MATSUMURA, AND HIDENOBU TANIHARA

• PURPOSE: To determine the risk factors for intraocular pressure (IOP) elevation after the injection of triamcinolone acetonide (TA).

• DESIGN: Retrospective interventional case-control study.

• METHODS: SETTING: Multicenter. PATIENT POPULATION: Four hundred and twenty-seven patients. OBSERVATION PROCEDURES: Intraocular pressure levels after TA treatment by the sub-Tenon capsule injection (STI; 12 mg, 20 mg, or 40 mg), intravitreal injection (IVI; 4 mg or 8 mg), or the combination of STI (20 mg) and IVI (4 mg), and IOP levels after two TA treatments. MAIN OUTCOME MEASURE: Risk factors for IOP levels of 24 mm Hg or higher.

• RESULTS: Younger age (hazards ratio [HR], 0.96/year; $P < .0001$), IVI (HR, 1.89/year; $P < .0001$), and higher baseline IOP (HR, 1.15/mm Hg; $P = .003$) were identified as risk factors. Dose dependency was shown in STI-treated eyes (HR, 1.07/mg; $P = .0006$), as well as after IVI (HR, 1.64/mg; $P = .013$). The combination of STI and IVI was a significant risk factor (HR, 2.27; $P = .003$) compared with STI alone. In eyes receiving two TA treatments, IVI (HR, 2.60; $P = .010$), higher IOP elevation after the first injection (HR, 1.18/mm Hg; $P = .011$), and increased dosage of STI (HR, 1.07/mm Hg; $P = .033$) were risk factors.

• CONCLUSIONS: Younger age, higher baseline IOP, IVI, and increased TA dosage were associated with TA-induced IOP elevation. IOP elevation after repeated TA injection was frequently associated with eyes treated with IVI, high IOP elevation after the first injection, and high doses of STI. (Am J Ophthalmol 2008; 145:676–681. © 2008 by Elsevier Inc. All rights reserved.)

Accepted for publication Dec 6, 2007.

From the Department of Ophthalmology and Visual Science, Kumamoto University Graduate School of Medical Sciences, Kumamoto, Japan (M.I., K.I., T.K., H.T.); Department of Ophthalmology and Visual Science, Nagoya City University Graduate School of Medical Sciences, Nagoya, Japan (Y.H., Y.O.); Department of Ophthalmology, Kagawa University Faculty of Medicine, Miki, Japan (K.H., F.S.); Department of Organs Therapeutics, Division of Ophthalmology, Kobe University Graduate School of Medicine, Kobe, Japan (Y.N., H.Y., A.N.); Department of Ophthalmology, Faculty of Medicine, Kagoshima University Graduate School of Medicine and Dental Sciences, Kagoshima, Japan (Y.S., T.S.); and Department of Ophthalmology, Kansai Medical University, Moriguchi, Japan (C.S., M.M.).

Inquiries to Masaru Inatani, Department of Ophthalmology and Visual Science, Kumamoto University Graduate School of Medical Sciences, 1-1-1, Honjo, 860-8556 Kumamoto, Japan; e-mail: inatani@fc.kuh.kumamoto-u.ac.jp

TRIAMCINOLONE ACETONIDE (TA) IS COMMONLY USED to treat various vitreoretinal diseases. TA limits the impact of corticosteroids on ocular tissues, thereby minimizing the side effects associated with systemic steroid therapy.[1–5] However, many patients who have received intravitreal injection (IVI) of TA or the sub-Tenon capsule injection of TA (STI) encounter intraocular pressure (IOP) elevation,[6–13] which can develop into glaucoma.[14,15] The prevalence of TA-induced IOP elevation is reportedly between 18% and 50%.[7,13,16–19] This wide range of values might be explained by the following: variation between definitions of IOP elevation; the TA dose and the method of administration; whether patients have previously received TA injections; patient background characteristics, including history of glaucoma or ocular hypertension; and administration of steroids. Several reports have suggested an increased prevalence of TA-induced IOP elevation in younger patients.[1,7,15,20] Therefore, we retrospectively investigated the risk factors for IOP elevation in patients receiving TA at six Japanese clinical centers, based on a standardized definition of TA-induced IOP elevation.

METHODS

• PATIENTS: We reviewed the medical records of patients receiving TA by STI (12 mg, 20 mg, or 40 mg), IVI (4 mg or 8 mg), or simultaneous administration by STI (20 mg) and IVI (4 mg) at the following six clinical centers in Japan: Kumamoto University Hospital (Kumamoto), Nagoya City University Hospital (Nagoya), Kagawa University Hospital (Miki), Kobe University Hospital (Kobe), Kagoshima University Hospital (Kagoshima), and Kansai Medical University Hospital (Moriguchi). Data from patients who received TA between April 1, 2002 and March 31, 2006 were included in the analyses. If both eyes were treated with TA, the eye that was treated first was

0002-9394/08/$34.00
doi:10.1016/j.ajo.2007.12.010

TABLE 1. Patient Data Before Triamcinolone Acetonide Treatment in < 24 mm Hg and ≥ 24 mm Hg Groups

Characteristic (n = 427)	Eyes with < 24 mm Hg (n = 377) n (%)	Eyes with ≥ 24 mm Hg (n = 50) n (%)	*p* value
Male gender	228 (60.5)	30 (60.0)	.948
Mean age (years)	65.8 ± 11.2	57.1 ± 17.5	.006*
Diabetes mellitus	203 (53.8)	17 (34.0)	.008*
Hypertension	137 (36.3)	18 (36.0)	.963
Cataract surgery	141 (37.4)	17 (34.0)	.636
Vitrectomy	88 (23.3)	14 (28.0)	.475
IVI included	69 (18.3)	25 (50.0)	<.0001*
Mean IOP at baseline (mm Hg)	13.8 ± 3.1	15.1 ± 3.1	.010*

IOP = intraocular pressure; IVI = intravitreal injection of triamcinolone acetonide.
*$P < .05$.

investigated. The exclusion criteria were as follows: eyes that had received intraocular surgery within three months before TA treatment; eyes with a history of glaucoma or uveitis; eyes that had shown > 21 mm Hg IOP levels; and patients who had been treated with steroids. Eyes treated with a second TA injection within the follow-up period were included in the analyses. If the TA dose administered in the second injection was different from that in the first, the eyes were included in the analysis of the first injection, but excluded from the analysis of the second.

• MAIN OUTCOME MEASURE AND OBSERVATION PROCEDURE: The main aim of this study was to investigate the risk factors for IOP elevation after TA treatment. The IOP levels after TA treatment were derived from patients' medical records. If any ocular surgeries were performed, IOP data from before the surgeries were evaluated. If an additional dose of TA was administered after the first injection, the IOP data at the first TA injection were evaluated until the second injection. The IOP levels were also evaluated between two weeks and a maximum of 12 months after the second injection. The baseline IOP was defined as the IOP level on the day of TA injection or at the last examination before the TA injection. The IOP data were mainly selected from records obtained by measurement using noncontact pneumotonometry. In line with previous reports,[6,15] we defined an IOP of 24 mm Hg or higher after TA treatment as elevated IOP induced by TA treatment. Furthermore, if IOP levels of 24 mm Hg or higher were shown by the noncontact pneumotonometer, they were re-examined using a Goldmann applanation tonometer on a slit-lamp biomicroscope, and the value shown by the tonometer was used as the IOP. Eyes for which the medical records did not indicate whether re-examination by tonometry had been performed were excluded from the study.

The following variables were assessed as potential risk factors for elevated IOP: gender; age; history of diabetes mellitus, hypertension, cataract surgery, or vitrectomy; dose and route of TA administration (12 mg, 20 mg, or 40 mg by STI; 4 mg or 8 mg by IVI; or a combination of 20 mg by STI and 4 mg by IVI); and baseline IOP. These factors were compared between patients with less than 24 mm Hg and those with 24 mm Hg or higher IOP. Potential risk factors for IOP levels of 24 mm Hg or higher after additional treatment were as described above. The maximal IOP minus baseline IOP (ΔIOP) values after the first treatment and the interval between the first and the second treatment were also assessed.

• STATISTICAL ANALYSIS: Data analysis was performed using the JMP version 6 statistical package program (SAS Institute, Cary, North Carolina, USA). The Mann–Whitney *U* test and the Chi-square test (or the Fisher exact test) were used for the univariate analyses. To confirm the effects of the risk factors and identify the hazard ratios (HRs) for TA-induced IOP elevation, multivariate Cox proportional hazards regression analysis was performed. The multivariate factors were selected from among the variants with a probability (*P*) value of less than .30 shown by univariate analysis. A *P* value less than .05 was considered statistically significant.

RESULTS

IN TOTAL, 427 EYES SATISFIED THE STUDY CRITERIA. ALL OF the eligible patients were Japanese. The diagnoses for the TA-treated eyes were as follows: age-related macular degeneration (67 eyes), other choroidal neovascular diseases (34 eyes), retinal vein occlusion (131 eyes), diabetic retinopathy (180 eyes), and other retinal diseases related to cystoid macular edema (15 eyes). Of these, 319 eyes were treated by one TA injection, and 108 eyes were treated with an additional TA injection. In total, 50 (11.7%) of the 427 eyes had an elevated IOP of 24 mm Hg or higher. IOP elevation of 24 mm Hg or above started 0.5

TABLE 2. Risk Factors for Elevated Intraocular Pressure Elevation of ≥ 24 mm Hg After Triamcinolone Acetonide Treatment—Cox Proportional Hazards Analysis

Variable	Hazards Ratio for ≥ 24 mm Hg	*p* value
Model 1: All eyes treated with triamcinolone acetonide injection (n = 427)		
Age (years)	0.96 (0.95 to 0.98)	<.0001*
Diabetes mellitus	0.76 (0.55 to 1.02)	.068
IVI included	1.89 (1.41 to 2.52)	<.0001*
IOP at baseline (mm Hg)	1.15 (1.05 to 1.27)	.003*
Model 2: Eyes with STI only (n = 333)		
Age (year)	0.96 (0.94 to 0.99)	.003*
Diabetes mellitus	0.91 (0.60 to 1.38)	.647
STI (mg)	1.07 (1.03 to 1.12)	.0006*
IOP at baseline (mm Hg)	1.31 (1.13–1.52)	.0003*
Model 3: Eyes with IVI only (n = 57)		
Age (year)	0.98 (0.94 to 1.03)	.393
Diabetes mellitus	0.91 (0.47 to 1.61)	.760
IVI (mg)	1.64 (1.09 to 3.39)	.013*
IOP at baseline (mm Hg)	1.03 (0.85 to 1.27)	.765
Model 4: Eyes with 20 mg of STI or 20 mg of STI plus 4 mg of IVI (n = 201)		
Age (year)	0.95 (0.92 to 0.98)	.003*
Diabetes mellitus	0.75 (0.41 to 1.29)	.306
Plus 4 mg of IVI	2.27 (1.33 to 4.02)	.003*
IOP at baseline (mm Hg)	1.28 (1.07 to 1.55)	.008*

IOP = intraocular pressure; IVI = intravitreal injection of triamcinolone acetonide; STI = sub-Tenon capsule injection of triamcinolone acetonide.
Hazards ratio is shown with 95% confidence interval.
*$P < .05$.

month after the injection in 12 eyes, after one month in nine eyes, after two months in 19 eyes, after three months in nine eyes, and after six months in one eye. Patient data before TA injection for the group with IOP elevation of less than 24 mm Hg and the group with 24 mm Hg or higher are shown in Table 1. The patients within the 24 mm Hg or higher group were younger, were less likely to have a history of diabetes mellitus, had a greater incidence of IVI administration of TA, and had higher baseline IOP values. The multivariate Cox proportional hazards regression showed that younger age (HR, 0.96 per year; 95% confidence interval [CI], 0.95 to 0.98; $P < .0001$), the inclusion of IVI (HR, 1.89; 95% CI, 1.41 to 2.52; $P < .0001$), and higher baseline IOP (HR, 1.15 per mm Hg; 95% CI, 1.05 to 1.27; $P = .003$) were risk factors for IOP elevation (Table 2; Model 1).

We also examined whether IOP elevation after TA injection was dose-dependent. In eyes treated by STI (n = 333), one of 36 eyes (2.8%), six of 164 eyes (3.7%), and 18 of 133 eyes (13.5%) showed IOP values of 24 mm Hg or higher after doses of 12 mg, 20 mg, and 40 mg by STI, respectively. Cox proportional hazards regression analysis of the 333 eyes identified younger age (HR, 0.96 per year; 95% CI, 0.94 to 0.99; $P = .003$), a higher dose administered by STI (HR, 1.07 per mg; 95% CI, 1.03 to 1.12; $P = .0006$), and higher baseline IOP (HR, 1.31 per mm Hg; 95% CI, 1.13 to 1.52; $P = .0003$) as risk factors (Table 2; Model 2). In eyes treated by IVI (n = 57), one of 18 eyes (5.6%) and 14 of 39 eyes (35.9%) were associated with IOP of 24 mm Hg or higher after doses of 4 mg and 8 mg by IVI, respectively. Cox proportional hazards regression analysis of the 57 eyes showed that a higher dose administered by IVI (HR, 1.64 per mg; 95% CI, 1.09 to 3.39; $P = .013$) was a risk factor. However, neither younger age (HR, 0.98 per year; 95% CI, 0.94 to 1.03; $P = .393$) nor higher baseline IOP (HR, 1.03 per mm Hg; 95% CI, 0.85 to 1.27; $P = .765$) were significant risk factors (Table 2; Model 3). Additionally, 10 of 37 eyes (27.0%) were associated with an IOP of 24 mm Hg or higher after simultaneous administration by STI (20 mg) and IVI (4 mg). In eyes treated with 20 mg by STI, or with both 20 mg by STI and 4 mg by IVI (n = 201), younger age (HR, 0.95 per year; 95% CI, 0.92 to 0.98; $P = .003$), the addition of 4 mg by IVI (HR, 2.27, 95% CI, 1.33 to 4.02; $P = .003$), and baseline IOP (HR, 1.28 per mm Hg; 95% CI, 1.07 to 1.55; $P = .008$) were identified as risk factors (Table 2; Model 4).

Of the 108 eyes treated with a second injection, 16 (14.8%) had IOP elevation to 24 mm Hg or higher. Data

TABLE 3. Data Before the Second Triamcinolone Acetonide Treatment in < 24 mm Hg and ≥ 24 mm Hg Groups

Characteristic (n = 108)	Eyes of < 24 mm Hg (n = 92) n (%)	Eyes of ≥ 24 mm Hg (n = 16) n (%)	*p* value
Male gender	53 (57.6)	10 (62.5)	.714
Mean age (years)	63.1 ± 11.0	55.6 ± 17.8	.279
Diabetes mellitus	50 (54.3)	8 (50.0)	.748
Hypertension	42 (45.7)	3 (18.8)	.044*
Cataract surgery	33 (35.9)	6 (37.5)	.900
Vitrectomy	24 (26.1)	5 (31.3)	.667
IVI included	4 (4.3)	4 (25.0)	.004*
Mean IOP at baseline (mm Hg)	13.8 ± 3.0	13.5 ± 2.4	.900
ΔIOP after the 1st injection (mm Hg)	3.0 ± 3.2	5.8 ± 2.1	<.0001*
Interval between 1st and 2nd injections (months)	5.2 ± 3.2	5.1 ± 3.2	.841

IOP = intraocular pressure; IVI = intravitreal injection of triamcinolone acetonide; ΔIOP = maximal IOP minus baseline IOP.

*$P < .05$.

TABLE 4. Risk Factors for Elevated Intraocular Pressure of ≥ 24 mm Hg After Second Triamcinolone Acetonide Injection—Cox Proportional Hazards Analysis

Variable (n = 108)	Hazards ratio for ≥ 24 mm Hg	*p* value
Model 1: All the eyes treated with repeated TA injections (n = 108)		
Age (years)	0.99 (0.95 to 1.02)	.410
Hypertension	0.71 (0.33 to 1.29)	.276
IVI included	2.60 (1.30 to 4.83)	.010*
ΔIOP after 1st injection (mm Hg)	1.18 (1.04 to 1.30)	.011*
Model 2: Eyes with repeated STIs (n = 100)		
Age (years)	1.03 (0.98 to 1.08)	.247
Hypertension	0.82 (0.37 to 1.58)	.557
STI (mg)	1.07 (1.01 to 1.18)	.033*
ΔIOP after 1st injection (mm Hg)	1.45 (1.17 to 1.85)	.0006*

IVI = intravitreal injection of triamcinolone acetonide; STI = sub-Tenon capsule injection of triamcinolone acetonide; ΔIOP = maximal IOP minus baseline IOP.

Hazards ratio is shown with 95% confidence interval.

*$P < .05$.

before the second TA treatment for the group with elevation of less than 24 mm Hg and the group with elevation of 24 mm Hg or higher are shown in Table 3. The 24 mm Hg or higher group included fewer patients with histories of hypertension, more eyes treated with the inclusion of IVI, and higher ΔIOP after the first injection. Cox proportional hazards regression analysis showed that the inclusion of IVI (HR, 2.60; 95% CI, 1.30 to 4.83; P = .010) and higher ΔIOP after the first injection (HR,1.18 per mm Hg; 95% CI, 1.04 to 1.30; P = .011) were risk factors for IOP elevation after the additional TA injection (Table 4; Model 1). In eyes treated with two STI injections (n = 100), an increased dose administered by STI (HR, 1.07 per mg; 95% CI, 1.01 to 1.18; P = .033) and higher ΔIOP after the first injection (HR, 1.45 per mm Hg; 95% CI, 1.17 to 1.85; P = .0006) were shown to be risk factors (Table 4; Model 2).

DISCUSSION

THIS STUDY INVESTIGATED THE RISK FACTORS OF IOP ELEvation following topical TA injection. Cox proportional hazards regression analysis of 427 eyes showed that younger age (HR, 0.96 per year; 95% CI, 0.95 to 0.98), TA treatment including IVI (HR, 1.89; 95% CI, 1.41 to 2.52), and higher baseline IOP (HR, 1.15 per year; 95% CI;1.05 to 1.27) were risk factors for elevated IOP of 24 mm Hg or

higher. These risk factors were also observed in the 201 eyes treated with either 20 mg by STI or a combination of 20 mg by STI and 4 mg by IVI. TA dose dependency for the frequency of IOP elevation was identified by multivariate analyses for 333 eyes treated by STI (1.07 per mg; 95% CI, 1.03 to 1.12) and 57 eyes treated by IVI (1.64 per mg; 95% CI, 1.09 to 3.39). Moreover, multivariate analyses in eyes after two TA treatments showed that TA treatment including IVI, higher ΔIOP after the first TA injection, and a higher dose administered by STI were risk factors.

Several reports have discussed the rates of IOP elevation after TA injection, and have identified potential risk factors. Retrospective studies examining IVI-induced IOP elevation reported that treatment with 20 mg by IVI induced IOP of more than 21 mm Hg in 112 of 272 patients (41.2%),[1] and that 4 mg by IVI induced IOP elevation by 30% or more in 267 of 528 eyes (50.6%),[12] IOP elevation to 24 mm Hg or higher in 36 of 89 patients (40.4%),[6] and IOP elevation to more than 21 mm Hg, or by more than 5 mm Hg, in 26 of 60 patients (43.3%).[20] These results indicate that higher baseline IOP values[6,12] and younger age[1,20] are risk factors for IVI-induced IOP elevation.

By contrast, retrospective studies of STI-induced IOP elevation showed levels equal to or more than 6 mm Hg, or IOP levels of more than 20 mm Hg, in nine of 49 eyes (18.4%),[13] and IOP elevation of equal to or more than 5 mm Hg in 19 of 43 eyes (44.2%).[8] In our previous retrospective study, 40 mg by STI induced high IOP of 24 mm Hg or above in 26 of 115 eyes (22.6%).[15] Younger age[15] and a history of diabetes mellitus[13] are reported risk factors for STI-induced IOP elevation. However, to determine in detail the influence of risk factors, including the dose and route of TA administration, it will be necessary to carry out statistical analysis on a larger number of eyes treated with TA at multiple clinical centers. In this meta-study, to determine the TA-induced IOP elevation more exactly, we excluded eyes with other risk factors for IOP elevation, such as glaucoma, ocular hypertension, uveitis, steroid administration, and recent histories of intraocular surgery. Moreover, TA-induced IOP elevation obtained using noncontact pneumotonometry was confirmed using a Goldmann applanation tonometer. Taken together, our retrospective results reflect the detailed characterization of TA-induced IOP elevation.

No previous large-scale clinical studies have confirmed the risk factors for TA-induced IOP, or examined the effects of the amount of TA administered and the interaction between STI and IVI. The present study not only confirmed that younger age and higher baseline IOP risk factors,[1,6,12,20] but also revealed that IVI induces IOP elevation more frequently than STI, as well as demonstrating the dose dependency for TA-induced IOP elevation. However, no correlations with gender, medical history of hypertension, diabetes mellitus, cataract surgery, or vitrectomy were observed in the analyses for the risk factors. Although some reports have shown that diabetes mellitus is a risk factor for corticosteroid-induced IOP elevation,[13,21] others have shown that it is not significant. A previous randomized diabetes mellitus clinical trial conducted by Palmberg[22] showed that the history of diabetes mellitus was not associated with glaucoma. Our results seem to agree with this. In addition, it could be speculated that the lens and the vitreous affect the diffusion of TA in the ocular tissue; however, no reports (including our present results) suggest that the histories of cataract surgery and vitreous surgery influence TA-induced ocular hypertension.

Interestingly, IVI and ΔIOP are risk factors for IOP elevation in eyes treated with repeated TA injections. IOP elevation is also frequently associated with a higher dose of repeated STI treatment. There are some reports concerning IOP elevation after repeated TA injection.[6,7,12] A study that retrospectively investigated 43 eyes treated repeatedly with 20 to 25 mg by IVI showed that no eyes with 21 mm Hg or less after the first TA injection exhibited more than 21 mm Hg after the second TA injection.[24] By contrast, another study previously reported that 28 of 43 eyes (65.1%) treated with a second TA injection showed an IOP elevation of 30% or more, which was not observed at the first TA injection.[12] In our present study, 15 of 16 eyes with IOP elevation after the second TA injection did not exhibit IOP elevation after the first TA injection. Our present data appear to agree with the latter study, although it showed that the risk factors for IOP elevation after the second TA injection were higher baseline IOP and male gender.[12]

The study presented here has several limitations. First, it shows the risk factors for IOP elevation and not for TA-induced visual field loss attributable to severe TA-induced ocular hypertension. We could not retrospectively quantify visual field loss in eyes with TA-induced IOP elevation because of the association with retinal macular diseases. Second, we did not statistically analyze the duration of IOP elevation in this study. In total, 44 of 50 eyes with IOP elevation in this study showed reversible IOP elevation, whereas six eyes were associated with persistent ocular hypertension in spite of anti-glaucomatous medical treatments. They were treated with trabeculectomy (two eyes) and trabeculotomy (four eyes), which is a surgical procedure effective for corticosteroid-induced glaucoma.[15,23] The six eyes included three treated with 8 mg by IVI, one treated with 4 mg by IVI, one treated with 4 mg by IVI plus 20 mg by STI, and one treated with 40 mg by STI. Persistent IOP elevation might be associated with IVI or high-dose treatment by STI. Third, it remains to be determined whether glaucoma and ocular hypertension are risk factors, as we excluded patients suffering from these disorders from the present study. Such patients might be more

susceptible to TA-induced IOP elevation. Actually, few cases with past histories of glaucoma and ocular hypertension were treated with TA injection. In our clinical centers, TA injection might have been avoided in the patients associated with glaucoma or ocular hypertension. Fourth, we could not evaluate worldwide differences as we only analyzed data from Japanese patients.

In conclusion, our case-control study indicates that younger patients, those with a higher baseline IOP, and those receiving higher doses of TA or intravitreally administered TA are more susceptible to corticosteroid-induced IOP elevation. Greater IOP elevation after the first injection is associated with frequent IOP elevations after the second TA injection.

THIS STUDY WAS SUPPORTED IN PART BY GRANTS-IN-AID FOR SCIENTIFIC RESEARCH FROM THE MINISTRY OF EDUCATION, Science, Sports, and Culture, Japan, and from the Ministry of Health and Welfare, Tokyo, Japan. The authors indicate no financial conflict of interest. Involved in design and conduct of study (M.I., K.I., H.T.); collection and management of the data (K.I., T.K., Y.H., Y.O., K.H., F.S., Y.N., H.Y., A.N., Y.S., T.S., C.S., M.M.); analysis (M.I., K.I.); interpretation of the data (M.I.); preparation of the first draft manuscript (M.I.), and in reviewing and approval of the manuscript (Y.O., F.S., A.N., T.S., M.M., H.T.). All procedures conformed to the Declaration of Helsinki and informed consent was obtained from each of the patients participating in the study. The retrospective interventional case-control study was approved by the Institutional Review Board of Kumamoto University Hospital (Kumamoto, Japan).

REFERENCES

1. Jonas JB, Kreissig I, Degenring R. Intravitreal triamcinolone acetonide for treatment of intraocular proliferative, exudative, and neovascular diseases. Prog Retin Eye Res 2005;24: 587–611.
2. Kawaji T, Hirata A, Awai N, et al. Trans-tenon retrobulbar triamcinolone injection for macular edema associated with branch retinal vein occlusion remaining after vitrectomy. Am J Ophthalmol 2005;140:540–542.
3. Antcliff RJ, Spalton DJ, Stanford MR, Graham EM, Ffytche TJ, Marshall J. Intravitreal triamcinolone for uveitic cystoid macular edema: an optical coherence tomography study. Ophthalmology 2001;108:765–772.
4. Danis RP, Ciulla TA, Pratt LM, Anliker W. Intravitreal triamcinolone acetonide in exudative age-related macular degeneration. Retina 2000;20:244–250.
5. Greenberg PB, Martidis A, Rogers AH, Duker JS, Reichel E. Intravitreal triamcinolone acetonide for macular edema due to central retinal vein occlusion. Br J Ophthalmol 2002;86: 247–248.
6. Smithen LM, Ober MD, Maranan L, Spaide RF. Intravitreal triamcinolone acetonide and intraocular pressure. Am J Ophthalmol 2004;138:740–743.
7. Jonas JB, Kreissig I, Degenring R. Intraocular pressure after intravitreal injection of triamcinolone acetonide. Br J Ophthalmol 2003;87:24–27.
8. Jea SY, Byon IS, Oum BS. Triamcinolone-induced intraocular pressure elevation: intravitreal injection for macular edema and posterior subtenon injection for uveitis. Korean J Ophthalmol 2006;20:99–103.
9. Benz MS, Albini TA, Holz ER, et al. Short-term course of intraocular pressure after intravitreal injection of triamcinolone acetonide. Ophthalmology 2006;113:1174–1178.
10. Ozkiris A, Erkilic K. Complications of intravitreal injection of triamcinolone acetonide. Can J Ophthalmol 2005;40:63–68.
11. Yamashita T, Uemura A, Kita H, Sakamoto T. Intraocular pressure after intravitreal injection of triamcinolone acetonide following vitrectomy for macular edema. J Glaucoma 2007;16:220–224.
12. Rhee DJ, Peck RE, Belmont J, et al. Intraocular pressure alterations following intravitreal triamcinolone acetonide. Br J Ophthalmol 2006;90:999–1003.
13. Hirooka K, Shiraga F, Tanaka S, Baba T, Mandai H. Risk factors for elevated intraocular pressure after trans-tenon retrobulbar injections of triamcinolone. Jpn J Ophthalmol 2006;50:235–238.
14. Kaushik S, Gupta V, Gupta A, Dogra MR, Singh R. Intractable glaucoma following intravitreal triamcinolone in central retinal vein occlusion. Am J Ophthalmol 2004;137: 758–760.
15. Iwao K, Inatani M, Kawaji T, Koga T, Mawatari Y, Tanihara H. Frequency and risk factors for intraocular pressure elevation after posterior sub-Tenon capsule triamcinolone acetonide injection. J Glaucoma 2007;16:251–256.
16. Bakri SJ, Beer PM. The effect of intravitreal triamcinolone acetonide on intraocular pressure. Ophthalmic Surg Lasers Imaging 2003;34:386–390.
17. Gillies MC, Simpson JM, Billson FA, et al. Safety of an intravitreal injection of triamcinolone: results from a randomized clinical trial. Arch Ophthalmol 2004;122: 336–340.
18. Park CH, Jaffe GJ, Fekrat S. Intravitreal triamcinolone acetonide in eyes with cystoid macular edema associated with central retinal vein occlusion. Am J Ophthalmol 2003;136: 419–425.
19. Massin P, Audren F, Haouchine B, et al. Intravitreal triamcinolone acetonide for diabetic diffuse macular edema: preliminary results of a prospective controlled trial. Ophthalmology 2004; 111:218–224.
20. Park HY, Yi K, Kim HK. Intraocular pressure elevation after intravitreal triamcinolone acetonide injection. Korean J Ophthalmol 2005;19:122–127.
21. Becker B, Bresnick G, Chevrette L, Kolker AE, Oaks MC, Cibis A. Intraocular pressure and its response to topical corticosteroids in diabetes. Arch Ophthalmol 1966;76:477–483.
22. Palmberg P. Screening for diabetic retinopathy. Diabetes Care 2001;24:419–420.
23. Honjo M, Tanihara H, Inatani M, Honda Y. External trabeculotomy for the treatment of steroid-induced glaucoma. J Glaucoma 2000;9:483–485.
24. Jonas JB, Degenring R, Kreissig I, Akkoyun I. Safety of intravitreal high-dose reinjections of triamcinolone acetonide. Am J Ophthalmol 2004;138:1054–1055.

nature biotechnology

Toward the generation of rod and cone photoreceptors from mouse, monkey and human embryonic stem cells

Fumitaka Osakada[1–4,7], Hanako Ikeda[1–3,5–7], Michiko Mandai[1,2], Takafumi Wataya[3], Kiichi Watanabe[3], Nagahisa Yoshimura[5], Akiori Akaike[4], Yoshiki Sasai[3] & Masayo Takahashi[1,2]

We previously reported the differentiation of mouse embryonic stem (ES) cells into retinal progenitors. However, these progenitors rarely differentiate into photoreceptors unless they are cultured with embryonic retinal tissues. Here we show the *in vitro* generation of putative rod and cone photoreceptors from mouse, monkey and human ES cells by stepwise treatments under defined culture conditions, in the absence of retinal tissues. With mouse ES cells, Crx$^+$ photoreceptor precursors were induced from Rx$^+$ retinal progenitors by treatment with a Notch signal inhibitor. Further application of fibroblast growth factors, Shh, taurine and retinoic acid yielded a greater number of rhodopsin$^+$ rod photoreceptors, in addition to default cone production. With monkey and human ES cells, feeder- and serum-free suspension culture combined with Wnt and Nodal inhibitors induced differentiation of Rx$^+$ or Mitf$^+$ retinal progenitors, which produced retinal pigment epithelial cells. Subsequent treatment with retinoic acid and taurine induced photoreceptor differentiation. These findings may facilitate the development of human ES cell–based transplantation therapies for retinal diseases.

Various ocular diseases, including retinitis pigmentosa, cone dystrophy and age-related macular degeneration, are characterized by a loss of photoreceptor cells, leading to blindness[1]. One promising therapeutic strategy is to transplant functional photoreceptor cells[2–6]. In addition to replacing photoreceptors, it may be important to regenerate retinal pigment epithelial (RPE) cells[4,5,7], which are essential for maintenance functions such as outer segment shedding, supplying nutrients to the retina and maintaining the blood-retinal barrier. However, a reliable, efficient method for producing large numbers of photoreceptors and RPE cells has not been devised. Specifically, a chemically defined culture method to efficiently generate photoreceptors from human ES cells would overcome a critical limitation for transplantation therapies.

Many groups, including ours, have attempted to generate photoreceptors *in vitro* from iris tissues[8,9], ciliary tissues[10] or ES cells[11–14]. Compared with tissue stem cells, ES cells are superior because their potential for infinite proliferation would permit production of a sufficient number of cells for research and treatment[15,16]. Retinal progenitors can be produced from ES cells *in vitro*[11–14], but generation of photoreceptors from these progenitors remains inefficient unless the cells are cocultured with developing retinal tissues. For instance, in our previous report[13], we induced neural retinal progenitors (~16%) from mouse ES cells using a serum-free floating culture of embryoid body–like aggregates (SFEB) system[17] combined with Dkk1, LeftyA, serum and activin treatment (SFEB/DLFA). However, in the absence of coculture with embryonic retinal tissues, differentiation of the retinal progenitors into photoreceptors was infrequent, suggesting that the proper inductive signals were missing in the culture. Here we searched for inductive conditions that would promote photoreceptor differentiation of ES cells. We report the efficient generation of putative photoreceptors from ES cells under defined culture conditions.

RESULTS

Differentiation of photoreceptor precursors from retinal progenitors

Neural retinal progenitors express the Rx (retinal homeobox) gene, which is essential for the specification of the eye field[18,19]. Using a mouse reporter ES cell line in which green fluorescent protein (GFP) is knocked in at the Rx locus of EB5 cells (Rx-KI cell line 116-18. T.W. and Y.S., unpublished data), we purified Rx$^+$ retinal progenitors (**Fig. 1**). ES cells were cultured under the SFEB/DLFA condition for 9 d, dissociated into single cells and sorted by fluorescence-activated cell sorting (FACS) (**Fig. 1a**). Consistent with our previous report[13], 15% of the SFEB/DLFA-treated ES cells were Rx-GFP$^+$ on day 9 (**Fig. 1b**). After a single sorting, >90% of the cells were GFP$^+$ (**Fig. 1c**). Immunostaining showed that most of the sorted cells (81.3 ± 1.4%) were Rx$^+$ and many of them (57.2 ± 1.8%) were Pax6$^+$, in accordance with the previous report[13] (**Supplementary Fig. 1** online).

In the first set of experiments, we tested whether the sorted cells differentiated towards photoreceptors. The cells were reaggregated by centrifugation[13], and the pelleted cells were replated on poly-D-lysine/

[1]Laboratory for Retinal Regeneration, Center for Developmental Biology, RIKEN, 2-2-3 Minatojima-minamimachi, Chuo-ku, Kobe, 650-0047, Japan. [2]Department of Experimental Therapeutics, Translational Research Center, Kyoto University Hospital, Kyoto, 606-8507, Japan. [3]Organogenesis and Neurogenesis Group, Center for Developmental Biology, RIKEN, Kobe, 650-0047, Japan. [4]Department of Pharmacology, Graduate School of Pharmaceutical Sciences, Kyoto University, Kyoto, 606-8501, Japan. [5]Department of Ophthalmology and Visual Sciences, Graduate School of Medicine, Kyoto University, Kyoto, 606-8507, Japan. [6]Shiga Medical Center for Adults, Moriyama, 524-8524, Japan. [7]These authors contributed equally to this work. Correspondence should be addressed to M.T. (mretina@cdb.riken.jp).

Received 11 May 2007; accepted 11 January 2008; published online 3 February 2008; doi:10.1038/nbt1384

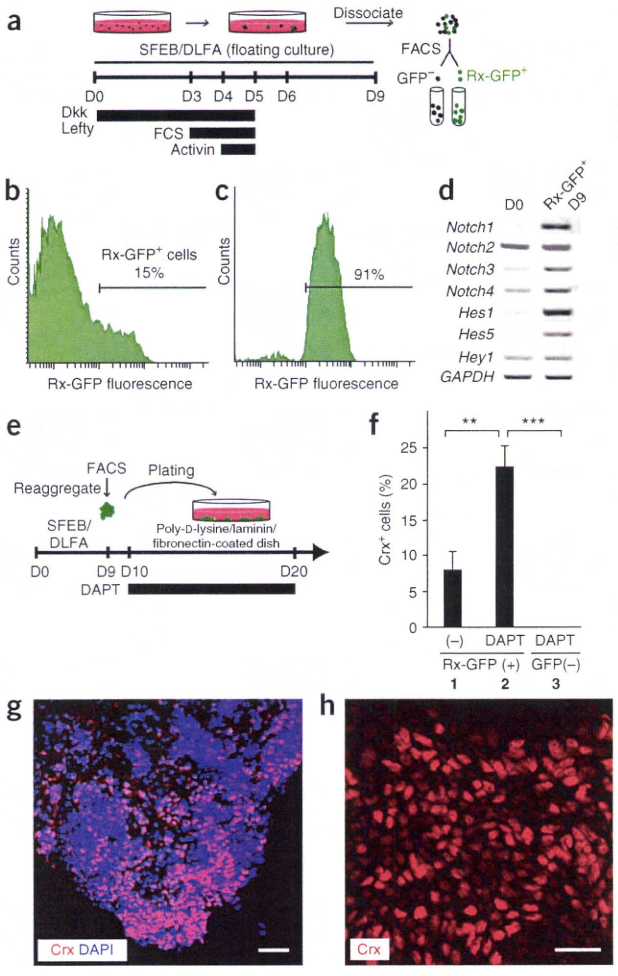

Figure 1 Efficient generation of photoreceptor precursors from FACS-purified ES cell–derived neural retinal progenitors using a γ-secretase inhibitor. (**a**) Schematic showing the procedure for the enrichment of Rx$^+$ retinal progenitors by FACS. D, culture day. (**b**,**c**) Flow-cytometry analyses of SFEB/DLFA-treated (on day 9) (**b**), or sorted Rx-GFP$^+$ cells (**c**). The percentage of Rx-GFP$^+$ cells is indicated. (**d**) RT-PCR analysis for genes involved in Notch signaling in the sorted Rx-GFP$^+$ (on day 9) or undifferentiated (D0) cells. (**e**) Schematic showing the procedure for photoreceptor-precursor differentiation from sorted Rx-GFP$^+$ cells. (**f**) Rx-GFP$^+$ cells were treated with and without DAPT, and Rx-GFP$^-$ cells were treated with DAPT from day 10, and the percentage of Crx$^+$ cells on day 20 was determined. $^{**}P < 0.01$, $^{***}P < 0.001$. (**g**,**h**) Immunocytochemical analyses of the sorted Rx-GFP$^+$ cells treated with DAPT, on day 20. Nuclei were counterstained with DAPI (**g**). Crx$^+$ cells were efficiently generated from the sorted cells (**h**). Scale bars, 100 μm (**g**) and 20 μm (**h**).

laminin/fibronectin-coated dishes (**Fig. 1e**). After an 11-d culture in differentiation medium[13] (that is, on differentiation day 20), a relatively small portion of the cells (7.8 ± 2.6%) was positive for Crx, a fate-determining factor for the photoreceptor lineage[20,21] (**Fig. 1f**, lane 1). This suggests that (i) the purified Rx$^+$ cells are competent to differentiate into photoreceptor precursors and (ii) the signals required for efficient photoreceptor differentiation are missing in this culture.

With this in mind, we investigated the role of Notch signaling, as inhibition of Notch signaling has been shown to promote photoreceptor differentiation both in organ culture[22] and *in vivo*[23,24]. Consistent with these reports, in our parallel study using organ culture, we observed that treatment of embryonic retinal tissues with the γ-secretase inhibitor DAPT (10 μM)[25,26] substantially increased the proportion of Crx$^+$ photoreceptor precursors and suppressed expression of the differentiation inhibitors Hes1 and Hes5 (**Supplementary Fig. 2** online). RT-PCR analysis showed that the purified Rx$^+$ cells expressed the Notch signaling components Notch1–4, Hes1, Hes5 and Hey1 (**Fig. 1d**). We examined the effect of Notch inhibition by culturing the ES cell–derived neural retinal progenitors in differentiation medium with or without DAPT (10 μM) (**Supplementary Fig. 3a** online). The frequency of Crx$^+$ cell aggregates was significantly increased by the DAPT treatment, and the DAPT treatment was most effective when applied on days 10–20 ($P < 0.01$, compared with no treatment) (**Supplementary Fig. 3b** online). At the cellular level, 22.4 ± 2.9% of the purified Rx-GFP$^+$ cells differentiated into Crx$^+$ photoreceptor precursors on day 20 under these conditions (**Fig. 1f–h**). In contrast, no Rx-GFP$^-$ cells expressed Crx (**Fig. 1f**). Although the differentiation efficiency varied between the cell lines, DAPT treatment also significantly increased the number of Crx$^+$ cells in another Rx-KI cell line, 20-10 (1.5 ± 0.7% in nontreated cells and 8.2 ± 1.9% in DAPT-treated cells; $P < 0.01$, an unpaired *t*-test). In the DAPT-treated cells, after photoreceptor-type cells, Mitf$^+$ (RPE progenitors) cells were most prominent (23.8 ± 2.7%) and Pax6$^+$-Islet1$^+$ (ganglion cells) cells were next (10.1 ± 1.7%). We also found calbindin$^+$ (mainly expressed in horizontal cells), HPC1$^+$ (mainly expressed in amacrine cells), PKC$^+$ (mainly expressed in bipolar cells) and cyclin D3$^+$ (immature Müller cells) cells (**Fig. 2a–f**). The proportion of Pax6$^+$/Islet1$^+$ or cyclin D3$^+$ cells increased with DAPT treatment. On the other hand, the proportion of calbindin$^+$, HPC1$^+$, PKC$^+$ or Mitf$^+$ cells did not change with the treatment (**Fig. 2a**).

Photoreceptor precursors express Crx just after they exit the cell cycle. Consistent with this, the ES cell–derived Crx$^+$ cells were negative for the mitotic marker Ki67 (**Supplementary Fig. 4a** online). We also examined 5-bromodeoxyuridine (BrdU) uptake and proliferating cell nuclear antigen (PCNA) expression in the induced Crx$^+$ cells. After 2 h of BrdU exposure, 99.3 ± 0.3% of Crx$^+$ cells were negative for BrdU uptake (**Supplementary Fig. 4b** online). Moreover, none of the Crx$^+$ cells were positive for PCNA (**Supplementary Fig. 4c** online). These results indicate that they were post-mitotic. We next analyzed the effects of DAPT on Ki67 expression and BrdU uptake (24 h) in the purified Rx$^+$ cells during differentiation days 11–20. On day 14 (after 4 d of treatment) and afterwards, the population of Ki67$^+$ cells in the DAPT-treated cells was smaller than in the untreated cells (**Supplementary Fig. 4d** online). Similarly, fewer BrdU$^+$ cells were observed among the DAPT-treated cells compared with the untreated controls on days 14–20 (**Supplementary Fig. 4e** online). These data show that DAPT treatment decreased the number of mitotic cells in the purified neural retinal progenitors. We then asked whether the decrease in mitotic cells by DAPT was caused by enhanced apoptosis (thereby excluding the mitotic cells) or by an increased number of cells differentiating into their post-mitotic state. During days 11–20, few of the Ki67$^+$ mitotic cells were positive for active caspase-3 (a marker for apoptotic cells). Moreover, the proportion of active caspase-3$^+$ cells was not significantly different between the DAPT-treated and untreated populations (**Supplementary Fig. 4f** online). Conversely, the cells treated with DAPT began to express Crx on differentiation day 16, and the proportion of Crx$^+$ cells gradually increased during days 16–20 (**Supplementary Fig. 3c** online). These

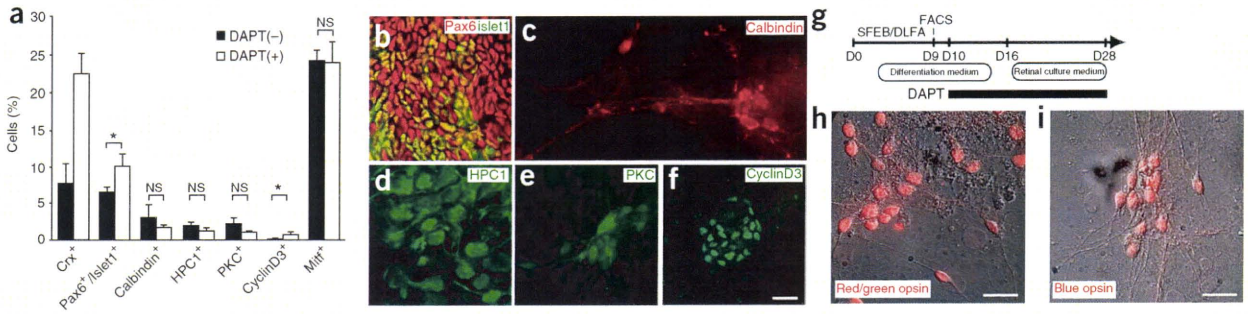

Figure 2 Effect of DAPT treatment on retinal cells. (**a**) The ratio of each type of retinal cells in the sorted cells treated with (white) or without (black) DAPT on day 20. $*P < 0.05$. (**b**–**f**) Immunostaining of DAPT-treated sorted cells on day 20. Images of Pax6$^+$/Islet1$^+$ ganglion cells (**b**), calbindin$^+$ mainly expressed in horizontal cells (**c**), HPC1$^+$ mainly expressed in amacrin cells (**d**), PKC$^+$ mainly expressed in bipolar cells (**e**) and cyclin D3$^+$ immature Müller cells (**f**). (**g**) Procedure for the differentiation of opsin$^+$ cone photoreceptors from mouse ES cells. FACS-purified Rx-GFP$^+$ cells were cultured for 19 d with DAPT. (**h**,**i**) Merged red/green-opsin (red) (**h**) or blue-opsin (red) (**i**) immunostaining and Nomarski images. Scale bar, 20 μm.

observations suggest that the γ-secretase inhibitor DAPT steers the mitotic retinal progenitors toward differentiation into post-mitotic photoreceptor precursors.

Differentiation of photoreceptors from photoreceptor precursors

Next, we examined whether the Crx$^+$ photoreceptor precursors could further differentiate into photoreceptors containing visual pigments. The purified ES cell–derived Rx$^+$ cells were cultured in differentiation medium containing DAPT from day 10, and then the medium was switched to retinal culture medium[13] on day 16 (around the time of onset of Crx expression, **Fig. 2g**). On day 28, immunostaining showed that 11.5 ± 2.0% and 10.7 ± 1.6% of the cells expressed red/green-opsin and blue-opsin, respectively (**Fig. 2h,i**); these are cone-specific pigment proteins that are indispensable for color vision. In contrast, fewer cells (5.5 ± 0.5%) expressed rhodopsin, the rod-type visual pigment.

To optimize the conditions for rod differentiation, we next tested several soluble factors that are reported to have positive effects on the genesis of rods from embryonic (or neonatal) retinal progenitors *in vitro*[27]. After FACS purification and DAPT treatment, each factor was first added individually to the retinal culture medium (**Fig. 3a**). Among these, acidic fibroblast growth factor (FGF) (50 ng/ml), basic FGF (10 ng/ml), taurine (1 mM)[28,29], Shh (3 nM) and retinoic acid (RA, 500 nM)[30] promoted rod differentiation (**Fig. 3b**). When these

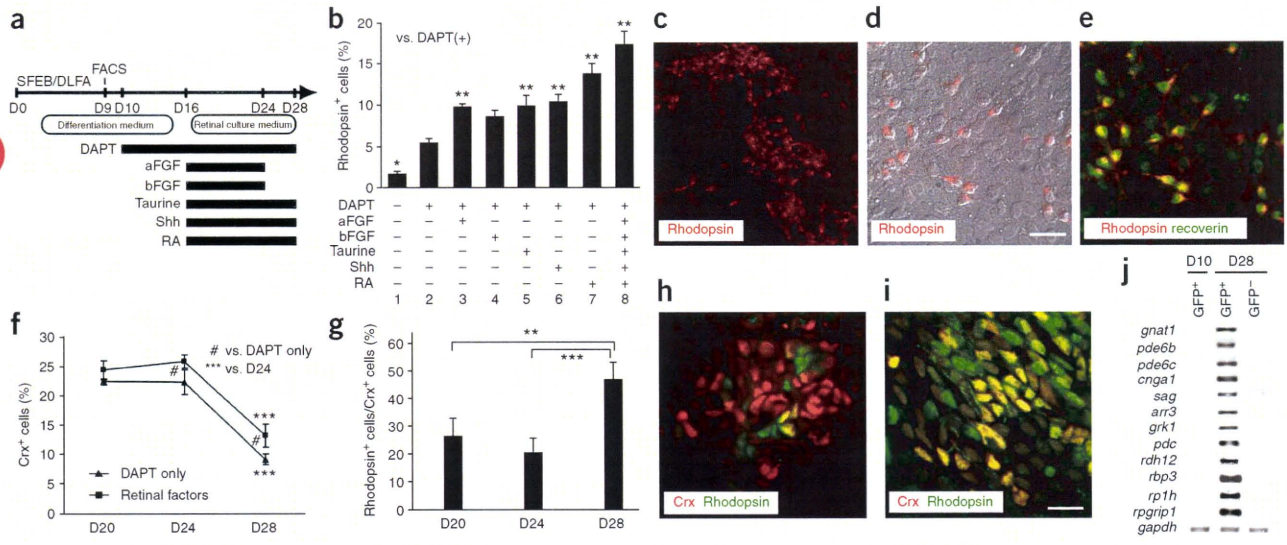

Figure 3 Promotion of rhodopsin$^+$ photoreceptor differentiation with FGFs, taurine, Shh and retinoic acid. (**a**) Procedure for the differentiation of rhodopsin$^+$ cells from ES cells. (**b**) Sorted Rx-GFP$^+$ cells were treated with the indicated factors on day 16, and the percentage of rhodopsin$^+$ cells on day 28 was determined. $*P < 0.05$, $**P < 0.01$, compared with DAPT (+) (lane 2). RA, retinoic acid. (**c**–**e**) Immunostaining of the sorted cells treated with DAPT, aFGF, bFGF, taurine, Shh and RA, on day 28. Many cells expressed rhodopsin (**c**). Merged view of rhodopsin staining (red) with Nomarski image (**d**) or with recoverin staining (green) (**e**). (**f**,**g**) Effect of retinal factors on Crx induction. (**f**) The percentages of Crx$^+$ cells in the DAPT-treated or DAPT- and retinal factors-treated cells on day 20-28. $\#P < 0.05$, $***P < 0.001$. (**g**) The percentages of rhodopsin$^+$/Crx$^+$ cells in the Crx$^+$ cells induced by retinal factors on days 20–28. $**P < 0.01$, $***P < 0.001$. (**h**,**i**) Coexpression of Crx and rhodopsin in the factor-treated Rx-GFP$^+$ cells on day 20 (**h**) and day 24 (**i**). Scale bar, 20 μm. (**j**) RT-PCR analysis for genes involved in phototransduction in the sorted Rx-GFP$^+$ (on day 10), the factor-treated Rx-GFP$^+$ (on day 28), or the factor-treated Rx-GFP$^-$ (on day 28) cells.

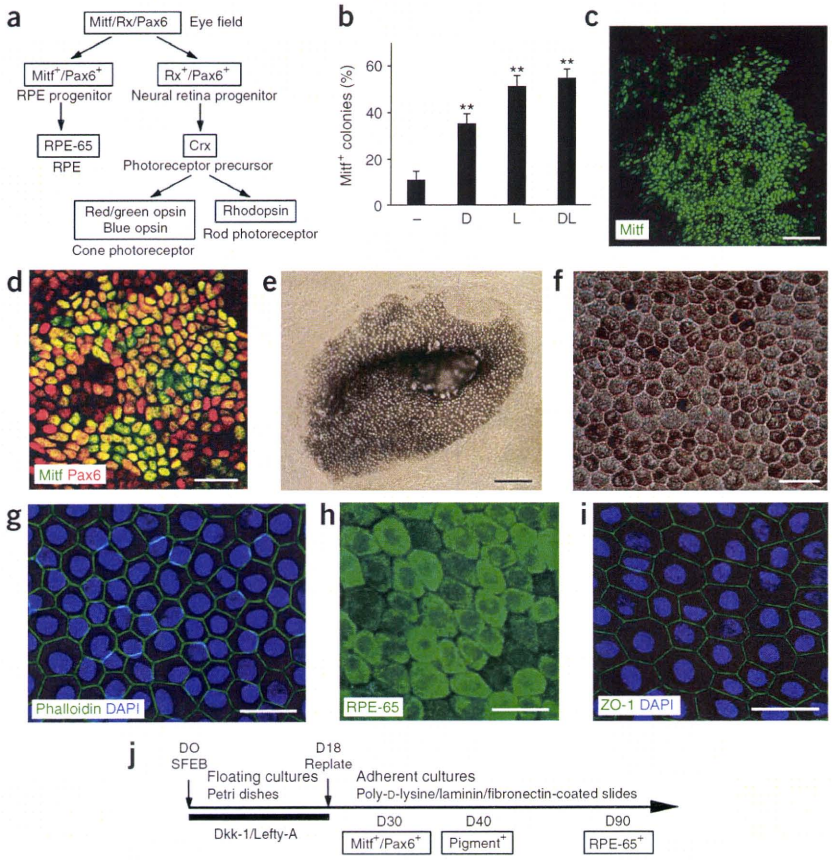

Figure 4 Directed differentiation of RPE cells from monkey ES cells in serum- and feeder-independent cultures. (**a**) Multiple-step commitment in the development of retinal cells. Markers for respective differentiation steps are boxed. (**b**) Percentages of Mitf$^+$ colonies in SFEB-treated ES cells. The SFEB culture combined with the application of Dkk-1 and Lefty-A produces the highest efficiency of differentiation of Mitf$^+$ colonies. ** $P < 0.01$, compared with SFEB alone. (**c**) SFEB/DL-treated monkey ES cells differentiate into Mitf$^+$ cells. (**d**) Generation of Mitf$^+$/Pax6$^+$ RPE progenitors from monkey ES cells in SFEB/DL cultures. (**e**) Phase-contrast images of pigment cells differentiated from monkey ES cells on day 40. (**f**) A high-magnification image of monkey ES cell–derived RPE cells in SFEB/DL cultures. Note that the pigmented cells display polygonal shapes. (**g**) Phalloidin staining shows polygonal shapes of RPE cells. (**h**) Monkey ES cell–derived pigment cells express RPE-65, a mature RPE-specific protein. (**i**) Formation of tight junctions, as determined by immunostaining with an anti-ZO-1 antibody. (**j**) Schema of RPE differentiation in SFEB/DL cultures. Scale bars, 100 μm (**c**,**e**), 30 μm (**d**), 20 μm (**f**–**i**).

factors were combined, 17.2 ± 1.8% of total cells expressed rhodopsin (**Fig. 3b–d**). These rhodopsin$^+$ cells coexpressed the photoreceptor marker recoverin[31] (**Fig. 3e**). These findings show that the combined treatment with FGFs, taurine, Shh and retinoic acid promotes the differentiation of ES cell–derived, DAPT-induced photoreceptor precursors towards rhodopsin$^+$-recoverin$^+$ rod photoreceptors. These factors had no effect on production of red/green-opsin$^+$ or the blue-opsin$^+$ cells (individually or combined; data not shown). Although the differentiation efficiency varied between cell lines, rhodopsin$^+$ cells (4.2% of total cells) were also induced by Rx-GFP sorting and subsequent treatment with DAPT and aFGF/bFGF/taurine/Shh/retinoic acid in another Rx-KI cell line, 20-10. Thus, we conclude that putative cone and rod photoreceptors can be selectively generated from ES cells *in vitro* using a stepwise treatment of defined soluble factors.

Although the sum of the induced red/green-opsin$^+$, blue-opsin$^+$ and rod-opsin$^+$ cells increased after treatment with soluble factors, the percentage of Crx$^+$ cells among the cells treated with these factors was only slightly higher than the proportion among nontreated cells on day 20 (22.5 ± 0.5% in nontreated cells, and 24.5 ± 1.6% in factor-treated cells) (**Fig. 3f**). The proportion of Crx$^+$ cells was almost the same on days 20 and 24, and decreased on day 28 (**Fig. 3f**). These results indicate that some overlap of the opsin staining existed on day 28. In fact, there is a report that certain photoreceptors express both red/green-opsin and blue-opsin in the mouse retina[32].

We also observed that there were cells expressing both Crx and rhodopsin in the factor-treated cells. On day 20, about 25% of Crx$^+$ cells expressed rhodopsin (6.0 ± 0.7% in total cells) (**Fig. 3g**,**h**). On day 28, about 45% of Crx$^+$ cells expressed rhodopsin (5.8 ± 0.5% in total cells) (**Fig. 3g**,**i**).

On day 28, the FACS-sorted, factor-treated cells expressed genes important for phototransduction in mature rods and/or cones—transducin-alpha (rod), phosphodiesterase (6b, rod; 6c, cone), cyclic nucleotide gated channel (a1, rod), arrestin (S-antigen, rod; arrestin3, cone), rhodopsin kinase (grk-1, rod), phosducin, retinol dehydrogenase and retinol binding protein—and genes specific to photoreceptors—rp1h and rpgrip (**Fig. 3j**). These data suggest that the cells have functional components for light responses.

Generation of RPE from monkey ES cells

In our established method (SFEB/DLFA) in mouse ES cells[13], differentiation into retinal cells requires fetal bovine serum (FBS), which is a disadvantage for transplantation therapies. We therefore searched for a method to generate retinal progenitors from monkey ES cells (CMK-6) using a defined culture system. Monkey ES cells were dissociated into small clumps of 5–10 cells and seeded in Petri dishes as suspension cultures with FBS-free differentiation medium. Under these conditions, monkey ES cells formed embryoid body–like aggregates. On day 18, these aggregates were plated onto poly-D-lysine/laminin/fibronection-coated slides. In vertebrates, the optic vesicle develops into the neural retina (inner layer) and the RPE (outer layer). Neural retinal progenitors express Rx[13,18,19], whereas the presumptive RPE expresses Mitf[13,33–35] (**Fig. 4a**). Therefore, we examined whether SFEB-treated monkey ES cells expressed these two markers. After 40 d in SFEB culture, a small percentage of colonies were Mitf$^+$ (~10%; **Fig. 4b**). We assessed the effects of soluble factors on the number of Mitf$^+$ colonies in SFEB cultures. Dkk-1, a Wnt antagonist, and Lefty-A, a nodal antagonist, both promote the differentiation of Rx$^+$ retinal progenitors from mouse ES cells[14]. Treating cultures with Dkk-1 (100 ng/ml) or Lefty-A (500 ng/ml) increased the percentage of Mitf$^+$ colonies to 35.3 ± 4.4% and 50.8 ± 5.0%,

respectively (**Fig. 4b**). Applying Dkk-1 and Lefty-A (SFEB/DL culture, hereafter) to cultures for 18 d provided a modest improvement over the results with Lefty-A alone (54.6 ± 4.2% of total colonies; **Fig. 4b,c**). SFEB/DL-treated Mitf$^+$ cells coexpressed Pax6 (90%; **Fig. 4d**), consistent with the *in vivo* marker profile of the embryonic RPE[13,33–35].

On day 40, pigmented cells were discernable under light microscopy in SFEB/DL cultures of monkey ES cells (**Fig. 4e**). Later, these cells accumulated more pigmentation and adopted a polygonal morphology with a squamous appearance (**Fig. 4f**). F-actin staining revealed the formation of polygonal actin bundles in these pigmented cells, a characteristic of the RPE[36] (**Fig. 4g**). On day 90, pigmented cells expressed RPE-65, a marker of the mature RPE (37.7 ± 3.9% of total cells; **Fig. 4h**), and ZO-1, a tight junction marker (40.1 ± 5.3% of total cells; **Fig. 4i**). Two independent ES cell lines (CMK-6 and CMK-9; normal karyotypes) provided similar results: Mitf$^+$ cells (50.8 ± 5.0% of colonies in CMK6; 43.2 ± 4.4% of colonies in CMK9) and pigmented cells (47.3 ± 3.7% of colonies in CMK6; 42.5 ± 4.9% of colonies in CMK9) (**Fig. 4j**). We conclude from these observations that monkey ES cell–derived pigment cells have typical features of the mature RPE.

Generation of photoreceptors from monkey ES cells

Next we investigated the generation of neural retinal progenitors from monkey ES cells under SEFB/DL conditions. On culture day 30, 42.5 ± 5.4% of the SFEB/DL-treated colonies expressed Rx, whereas 17.5 ± 3.1% of the SFEB-treated colonies were Rx$^+$ (**Fig. 5a,b**). Most Rx$^+$ cells in the SFEB/DL cultures were also Pax6$^+$ (**Fig. 5c**), consistent with the marker profile of neural retinal progenitors[13]. The induced Rx$^+$ cells were frequently found in close proximity to Mitf$^+$ cell clusters. Thus, SFEB/DL treatment induces ES cells to differentiate into cells with characteristics of retinal progenitors.

Subsequently, we examined the differentiation *in vitro* of monkey ES cells into photoreceptors. After 90 d of SFEB culture, only 6.7 ± 3.1% of colonies expressed Crx[20,21] (**Fig. 5d**), whereas 24.2 ± 3.8% of SFEB/DL-treated colonies were Crx$^+$ (**Fig. 5d**). To establish a chemically defined culture for photoreceptor differentiation, we applied two of the compounds that promote differentiation of rod photoreceptors in mouse ES cell cultures, retinoic acid and taurine (**Fig. 3a,b**). On and after day 90, SFEB/DL-treated ES cells were incubated in FBS-free medium containing retinoic acid (1 μM), taurine (100 μM) and N2 supplement (RA/T medium). On day 120, 28.5 ± 3.6% of colonies were Crx$^+$ in SFEB/DL + RA/T cultures. Notably, 71.0 ± 5.4% of cells in the Crx$^+$ colonies expressed Crx by day 120 (24.0 ± 4.4% of total cells), compared with only 43.2 ± 6.3% of cells without RA/T treatment (9.2 ± 3.0% of total cells) (**Fig. 5e–g**). This extensive induction of Crx$^+$ expression has not been reported for other ES cell differentiation systems.

We examined the expression of the rod photoreceptor marker rhodopsin in SFEB/DL cultures. Rhodopsin$^+$ cells were evident in these cultures on day 130 (20.7 ± 4.4% of colonies), but were rarely observed in SEFB cultures (**Fig. 5h**). To promote photoreceptor differentiation, we used treatment with RA/T. On day 130, 27.5 ± 3.6% of colonies were rhodopsin$^+$ in SFEB/DL + RA/T cultures. RA/T treatment significantly increased the percentage of rhodopsin$^+$ cells in SFEB/DL-treated cultures (3.8 ± 1.5% of total cells in SFEB/DL cultures; 12.1 ± 3.4% of total cells in SFEB/DL + RA/T cultures, $P < 0.001$) (**Fig. 5i–k**). Most of the rhodopsin$^+$ cells coexpressed Crx and recoverin[31] (**Fig. 5l**). The SFEB/DL + RA/T method also induced

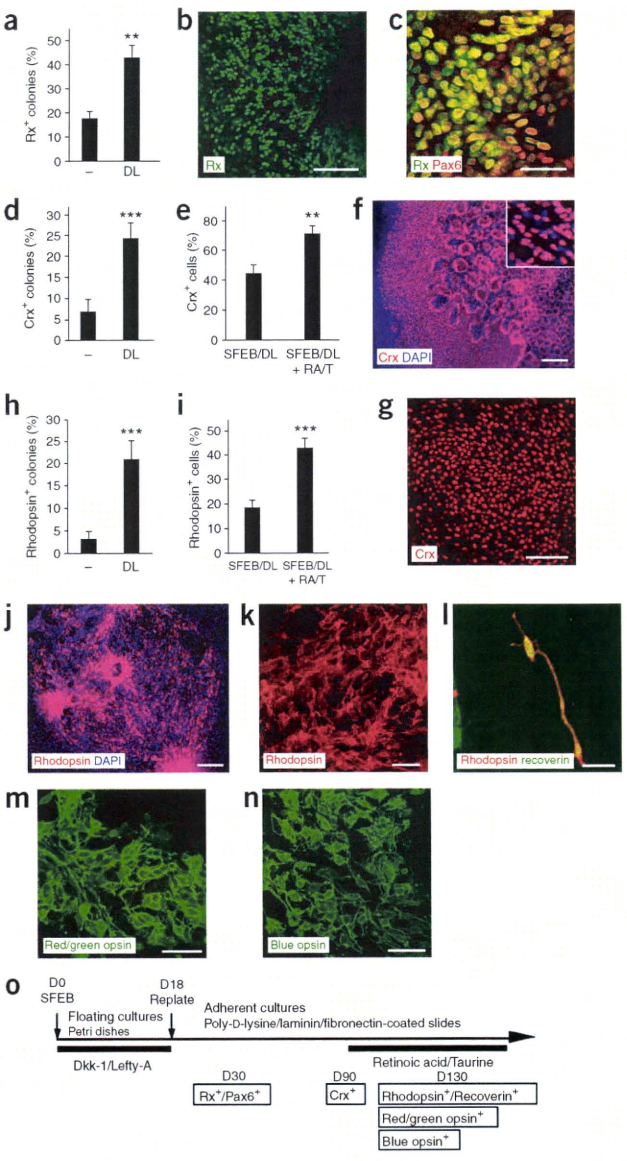

Figure 5 Retinoic acid and taurine promote differentiation into photoreceptor cells. (**a**) Dkk-1 and Lefty-A increase the percentage of Rx$^+$ colonies in SFEB cultures. ** $P < 0.01$, compared with SFEB alone. (**b**) Efficient differentiation of Rx$^+$ colonies from SFEB/DL-treated ES cells. (**c**) Generation of Rx$^+$/Pax6$^+$ neural retina progenitors from monkey ES cells in SFEB/DL cultures. (**d**) SFEB/DL treatment increases the percentage of Crx$^+$ colonies. *** $P < 0.001$, compared with SFEB alone. (**e**) RA/T treatment increases the percentage of Crx$^+$ cells within Crx$^+$ colonies. ** $P < 0.01$, compared with SFEB/DL alone. (**f,g**) Differentiation of Crx$^+$ photoreceptor precursors from SFEB/DL and RA/T-treated monkey ES cells. (**h**) SFEB/DL treatment increases the percentage of rhodopsin$^+$ colonies. *** $P < 0.001$, compared with SFEB alone. (**i**) RA/T treatment increases the percentage of rhodopsin$^+$ cells within rhodopsin$^+$ colonies. *** $P < 0.001$, compared with SFEB/DL alone. (**j,k**) Differentiation of rhodopsin$^+$ rod photoreceptors from SFEB/DL and RA/T-treated monkey ES cells. (**l**) Monkey ES cell–derived rhodopsin$^+$ cells coexpress recoverin. (**m,n**) Monkey ES cells differentiate into red/green opsin$^+$ (**m**) or blue opsin$^+$ (**n**) cone photoreceptors in SFEB/DL + RA/T cultures. (**o**) Schema of photoreceptor differentiation in SFEB/DL and RA/T cultures. Scale bars, 100 μm (**b,f,g,j**), 30 μm (**c,k,m,n**), 10 μm (**l**).

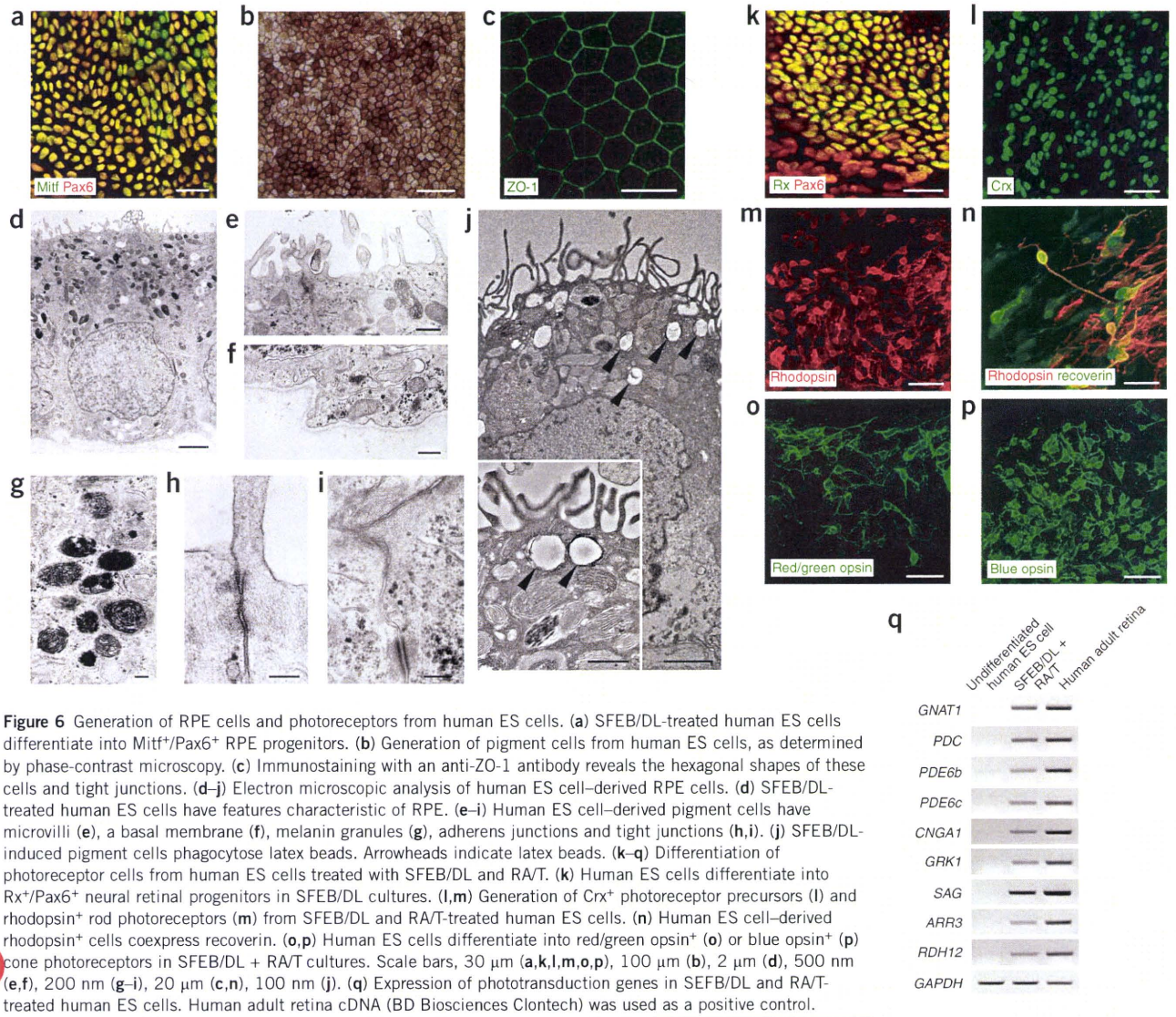

Figure 6 Generation of RPE cells and photoreceptors from human ES cells. (**a**) SFEB/DL-treated human ES cells differentiate into Mitf$^+$/Pax6$^+$ RPE progenitors. (**b**) Generation of pigment cells from human ES cells, as determined by phase-contrast microscopy. (**c**) Immunostaining with an anti-ZO-1 antibody reveals the hexagonal shapes of these cells and tight junctions. (**d–j**) Electron microscopic analysis of human ES cell–derived RPE cells. (**d**) SFEB/DL-treated human ES cells have features characteristic of RPE. (**e–i**) Human ES cell–derived pigment cells have microvilli (**e**), a basal membrane (**f**), melanin granules (**g**), adherens junctions and tight junctions (**h**,**i**). (**j**) SFEB/DL-induced pigment cells phagocytose latex beads. Arrowheads indicate latex beads. (**k–q**) Differentiation of photoreceptor cells from human ES cells treated with SFEB/DL and RA/T. (**k**) Human ES cells differentiate into Rx$^+$/Pax6$^+$ neural retinal progenitors in SFEB/DL cultures. (**l**,**m**) Generation of Crx$^+$ photoreceptor precursors (**l**) and rhodopsin$^+$ rod photoreceptors (**m**) from SFEB/DL and RA/T-treated human ES cells. (**n**) Human ES cell–derived rhodopsin$^+$ cells coexpress recoverin. (**o**,**p**) Human ES cells differentiate into red/green opsin$^+$ (**o**) or blue opsin$^+$ (**p**) cone photoreceptors in SFEB/DL + RA/T cultures. Scale bars, 30 μm (**a**,**k**,**l**,**m**,**o**,**p**), 100 μm (**b**), 2 μm (**d**), 500 nm (**e**,**f**), 200 nm (**g–i**), 20 μm (**c**,**n**), 100 nm (**j**). (**q**) Expression of phototransduction genes in SEFB/DL and RA/T-treated human ES cells. Human adult retina cDNA (BD Biosciences Clontech) was used as a positive control.

differentiation of monkey ES cells into red/green opsin$^+$ (30.1 ± 3.7% of colonies; 12.8 ± 3.5% of total cells; **Fig. 5m**) or blue opsin$^+$ (34.5 ± 4.1% of colonies; 13.9 ± 3.0% of total cells; **Fig. 5n**) cone photoreceptor cells. Notably, ~35% of total cells were photoreceptor-like cells under this method. In another cell line (CMK-9), the SFEB/DL + RA/T method also induced rhodopsin$^+$ cells (24.8 ± 2.7% of colonies (**Fig. 5**)). In addition to photoreceptor cells, we observed other retinal neurons in these culture conditions at low efficiency including HPC1$^+$/Pax6$^+$ amacrine cells, PKCα$^+$ bipolar cells, Pax6$^+$-Islet1/2$^+$ ganglion cells and glutamine synthase$^+$ Müller cells (**Supplementary Fig. 5** online). These induced retinal cells were frequently found in the same clusters. Thus, we conclude that SFEB/DL + RA/T treatment efficiently generates rod and cone photoreceptor cells from monkey ES cells.

Generation of RPE and photoreceptors from human ES cells

In the final set of experiments, we examined whether human ES cells (khES-1) can differentiate into retinal cells under defined culture conditions. We optimized the SFEB culture for human ES cells. Human ES cells were dissociated into cell clumps (5–10 cells per clump) in FBS-free differentiation medium, and both the WNT antagonist DKK-1 (100 ng/ml) and the NODAL antagonist LEFTY-A (500 ng/ml) were applied for the first 20 d of suspension culture. Subsequently, ES cell aggregates were replated onto poly-D-lysine/laminin/fibronectin-coated slides. First, we examined the differentiation of human ES cells into RPE cells. On day 50, Mitf$^+$-Pax6$^+$ colonies were abundant (30.6 ± 4.7% of colonies; **Fig. 6a**). A number of pigment cells with squamous and hexagonal morphology were present in these SFEB/DL-treated human ES cell cultures on day 60 (37.4 ± 4.6% of colonies; **Fig. 6b**). Immunostaining with an anti-ZO-1 antibody revealed that pigment cells derived from human ES cells formed tight junctions by day 120 (34.7 ± 4.0% of total cells; **Fig. 6c**). To determine whether the SFEB/DL-induced pigmented cells have structural characteristics of the RPE, we studied electron micrographs of these cells. ES cell–derived pigmented cells were polarized, with apical microvilli (**Fig. 6d**,**e**) and basal membranes (**Fig. 6d**,**f**). Melanin

granules were abundant in the cytoplasm, predominantly in the apical and mid-portions of the cell, but were absent from the basal cytoplasm (**Fig. 6d**). These are characteristics of mature human RPE[37]. Melanin granules of different maturity were present in the ES cell–derived pigmented cells (**Fig. 6g**). The presence of tight junctions and adherens junctions was also confirmed by electron microscopy (**Fig. 6h,i**). Phagocytosis is an important function of the RPE and required for the maintenance of photoreceptor functions. Electron microscopy showed that the SFEB/DL-induced pigmented cells incorporated latex beads (**Fig. 6j**). From these findings, we conclude that human ES cells differentiate into cells with typical RPE characteristics in SFEB/DL culture.

We then examined differentiation into photoreceptor cells. Rx^+ cells were present in SFEB/DL culture on day 25, whereas no Rx^+ colonies were observed in SFEB culture. On day 35, 15.8 ± 2.5% of colonies were Rx^+-$Pax6^+$ (**Fig. 6k**). Thus, SFEB/DL treatment induces differentiation of human ES cells into neural retinal progenitors. Next, we determined whether SFEB/DL-induced retinal progenitors can differentiate into photoreceptor cells under RA/T conditions. On day 90, a few Crx^+ cells were observed in SEFB/DL cultures. Crx^+ photoreceptor precursors increased under SEFB/DL and RA/T conditions as the culture period was extended: 11.3 ± 1.9% of total cells on day 120, and 19.6 ± 4.1% of total cells on day 170 (**Fig. 6l**). Rhodopsin$^+$ rod photoreceptors were present by day 130. The number of rhodopsin$^+$ cells increased in SEFB/DL and RA/T cultures to 5.1 ± 0.8% and 8.5 ± 2.9% of total cells on day 150 and day 200, respectively (**Fig. 6m**). These rhodopsin$^+$ cells coexpressed recoverin (**Fig. 6n**). Red/green opsin$^+$ (21.4 ± 4.0% of colonies, 8.9 ± 3.4% of total cells; **Fig. 6o**) or blue opsin$^+$ (23.9 ± 3.7% of colonies, 9.4 ± 3.6% of total cells; **Fig. 6p**) cone photoreceptors were also observed in SFEB/DL + RA/T cultures. The rhodopsin$^+$ cells were found in close proximity to red/green opsin$^+$ or blue opsin$^+$ cells in the same clusters. We confirmed that our method induced retinal differentiation in two independent human ES cell lines (khES1 and khES3; normal karyotypes): $Mitf^+$ cells (30.6 ± 4.7% of colonies in khES1; 34.7 ± 3.0% of colonies in khES3) and rhodopsin$^+$ cells (14.3 ± 4.2% of colonies in khES1; 11.3 ± 2.1% of colonies in khES3). SFEB/DL and RA/T-treated cells expressed genes responsible for phototransduction in rods and/or cones: transducin-alpha (rod), phosducin (rod and cone), phosphodiesterase (6b, rod; 6c, cone), cyclic nucleotide gated channel (a1, rod), rhodopsin kinase (grk-1, rod), arrestin S-antigen (rod), arrestin3 (cone), retinol dehydrogenase (rod and cone) on days 140–200 (**Fig. 6q**). These results indicate that human ES cell–derived photoreceptor cells have functional components for light responses. Thus, we conclude that human ES cells treated with SFEB/DL generate retinal progenitors, which differentiate into putative photoreceptor cells in RA/T culture conditions.

DISCUSSION

The potential of retinal cell transplantation to restore visual function has been demonstrated using animal models[4,6], and a clinical trial is under way for retinitis pigmentosa using fetal retinas[5]. However, use of the fetal retina involves some ethical and practical considerations. Photoreceptors or RPE cells derived from human ES cells could address the problem of cell supply. With respect to retinal degenerative diseases, *in vitro* generation of rod photoreceptors is particularly valuable, as ~95% of the photoreceptors in humans are of the rod type, and they are the receptors predominantly lost in individuals with retinitis pigmentosa. Although immature cells like those in the fetal retina were originally thought to be ideal for transplantation, more rhodopsin$^+$ cells survive in the host retina when the more mature P5 rather than the immature P1 mouse retinal cells are transplanted[6]. Thus, transplantation may be more successful if photoreceptor cell differentiation is induced before transplantation.

Human ES cells cultured on mouse feeder cells express an immunogenic nonhuman sialic acid on their surface[38]. Thus, clinical application of human ES cells requires elimination of animal-derived substances. To our knowledge, no previous report has produced photoreceptor cells in uncontaminated culture conditions. We have generated retinal progenitors in the presence of FBS[13], and another group generated retinal progenitors from human ES cells using Matrigel, a material derived from mouse sarcoma that has not been completely characterized and may contain xenogenic contaminants[14]. The present study demonstrates the *in vitro* generation of photoreceptors from human ES cells under defined culture conditions free of animal-derived substances. Moreover, the differentiation of photoreceptors from monkey and human ES cells is relatively efficient (25–35%) compared with previous work (e.g., ref. 14 induced Crx^+ photoreceptor precursors at 12% and photoreceptors at <0.01%).

One important observation in this study is that the FACS-purified Rx^+ mouse cells before DAPT treatment remained mitotic for a considerable period (**Supplementary Fig. 4d,e** online), yet DAPT-treated cells never formed tumors after transplantation (data not shown), raising the possibility that the number of purified neural retinal progenitor cells may be increased before using them for further studies. This could be a advantage for this system in future transplantation studies as well as in screens for factors that promote photoreceptor differentiation and survival.

For a comprehensive functional analysis of the ES cell–derived retinal cells in transplantation studies, we have three problems to solve: (i) devising a selection system to purify photoreceptors, RPE cells or their precursors, (ii) managing a long culture period for generating mature retinal cells, and (iii) overcoming host microenvironment obstacles, such as the glial barrier. In mouse ES cell cultures, we have shown here that a Notch inhibitor promotes photoreceptor differentiation in FACS-purified Rx^+ cells, although it has no effect on Rx^+ cells present in unpurified SFEB-treated cells. It may be possible to obtain a greater number of photoreceptor cells in a shorter period of time by applying this selection and subsequent induction of differentiation to human ES cells. We cocultured mouse ES cell–derived photoreceptors with the P8 mouse retina. These cells survived in the host retina, expressed rhodopsin and integrated into the outer nuclear layer, where endogenous photoreceptors are located (**Supplementary Fig. 6** online). These results indicate that ES cell–derived rhodopsin$^+$ cells are preferentially incorporated into the proper layer for photoreceptors. In addition, two weeks after *in vivo* subretinal transplantation in the rat, a few cells survived in the host retina, and expressed rhodopsin (data not shown). Although these observations are promising, the number of surviving cells in the retina was low (<0.5% of the grafted cells), indicating that substantial host microenvironmental problems must be solved before functional studies will be successful. Studies of facilitated cell survival and tissue integration will be particularly important. Further research is warranted to establish selection methods, analyze photoreceptor functions and transplant human ES cell–derived retinal cells in animal models of retinal degeneration.

Several lines of evidence indicate that transplantation of both neural retinal and RPE tissues improves vision in animals[4] and humans[5], suggesting that combined transplantation of human ES cell–derived photoreceptors and RPE cells may be most effective. Thorough testing of these approaches in relevant animal models is essential, and our

method should facilitate monkey allograft transplantation experiments with monkey ES cell–derived photoreceptors and RPE cells. Moreover, it could be applied to induced pluripotent stem (iPS) cells generated from adult human somatic cells[39]. Finally, our differentiation system and the resulting cells may be useful for testing drugs[40] and for studying the development of the human central nervous system, especially the eye.

METHODS

Mouse ES cells. The methods for mouse ES cell maintenance and differentiation in SFEB culture have been described previously[13,17]. For the SFEB/DLFA method, Dkk1 (100 ng/ml, during days 0–5, R&D Systems), LeftyA (500 ng/ml, during days 0–5, R&D Systems), 5% FBS (during days 3–5, JRH Biosciences) and activin-A (10 ng/ml, during days 4–5, R&D Systems) were added to the differentiation medium (G-MEM, 5% knockout serum replacement (KSR); GIBCO), 0.1 mM nonessential amino acids, 1 mM pyruvate and 0.1 mM 2-mercaptoethanol).

For FACS (see below), the cell aggregates were incubated in suspension culture in differentiation medium until day 9. After FACS, 1–2 × 104 sorted cells were resuspended in differentiation medium containing 10% FBS, and spun for 10 min at 800*g* to produce a reaggregation pellet. After 1 h of culture at 37 °C, 3–5 reaggregated pellets cm^{-2} were replated, dishes coated with poly-D-lysine (BD BioCoat), laminin (3 μg/cm^2, BD) and fibronectin (1 μg/cm^2, GIBCO) with differentiation medium supplemented with 10% FBS. On day 10, the culture medium was changed to differentiation medium without FBS and with or without a γ-secretase inhibitor, N-[N-(3,5-difluorophenacetyl)-L-alanyl]-S-phenylglycine t-butyl ester (DAPT, 10 μM, Calbiochem).

For photoreceptor differentiation, the medium was changed to retinal culture medium (66% E-MEM-HEPES (Sigma), 33% HBSS (GIBCO), 1% FCS supplemented with N2 supplement (GIBCO), 5.75 mg/ml glucose, 200 μM L-glutamine, 100 U/ml penicillin and 100 μg/ml streptomycin)[13] with the factors indicated in **Figure 3a**, on day 16. aFGF (R&D Systems) and bFGF (R&D Systems) were added during differentiation days 16–24, and taurine (Sigma), Shh (R&D Systems) and retinoic acid (Sigma) were added during days 16–28. The medium was changed every other day. Two independent lines of Rx-KI ES cells (116-18 and 20-10) differentiated into Crx^+ photoreceptor precursors and $rhodopsin^+$ rod photoreceptors by Rx-GFP sorting and subsequent treatment with DAPT and aFGF/bFGF/taurine/Shh/retinoic acid.

Monkey ES cells. Two independent lines of cynomolgus monkey ES cells (CMK-6 and CMK-9) were maintained as previously described[7,41,42]. In brief, undifferentiated monkey ES cells were maintained on a feeder layer of mitomycin C–treated mouse embryonic fibroblasts (STO cells). STO cells were incubated with 10 μg/ml mitomycin C (Wako) for 2 h and plated on a gelatin-coated dish. Undifferentiated monkey ES cells were incubated in DMEM/F-12 (Sigma) supplemented with 0.1 mM 2-mercaptoethanol (Sigma), 0.1 mM nonessential amino acids (Sigma), 2 mM L-glutamine (Sigma), 20% KSR, 1,000 units/ml leukemia inhibitory factor (ESGRO; Chemicon), and 4 ng/ml bFGF (Upstate Biotechnology). ES cells were passaged with 0.25% trypsin (GIBCO) in PBS with 1 mM $CaCl_2$ and 20% KSR every 3 d. For storage, the monkey ES colonies were suspended in ice-cold culture medium supplemented with 2M DMSO, 1M acetamide and 3M polypropylene glycol, and quickly frozen with liquid N2. The monkey ES cell lines used in this study formed tightly packed colonies with each cell exhibiting a high nuclear/cytoplasmic ratio. These cells expressed undifferentiated ES cell markers such as Oct-3/4 and Nanog, but not pan-neural markers such as nestin, βIII-tubulin and microtubule-associated protein-2(a+b), even after being maintained in culture for more than 1 year. Therefore, these ES cells remained undifferentiated in our cultures.

To induce differentiation, ES colonies were partially dissociated into clumps (5–10 cells per clump) with 0.25% trypsin in PBS with 1 mM $CaCl_2$ and 20% KSR. It should be noted that the efficiency of neural induction was low if the ES clumps were too large. STO feeders were removed by incubation of the ES clumps on a gelatin-coated dish for 30 min. ES clumps at a density of 6.7 × 10^3 ES clumps/ml were incubated in a nonadhesive bacterial-grade dish with ES differentiation medium (G-MEM, 10% KSR, 0.1 mM nonessential amino acids, 1 mM pyruvate and 0.1 mM 2-mercaptoethanol). Recombinant Dkk-1 protein (100 ng/ml) and Lefty-A protein (500 ng/ml) were added to the differentiation medium of the suspension culture for 18 d. Thereafter, ES cell aggregates that spontaneously formed were replated *en bloc* at a density of 10–15 aggregates per cm^2 on poly-D-lysine/laminin/fibronectin-coated 8-well culture slides.

To generate photoreceptor cells, we further incubated SFEB/DL-treated differentiated cells in the RA/T medium (GMEM + 5% KSR + N2 supplement + retinoic acid (1 μM) + taurine (100 μM) + penicillin (100 units/ml)/streptomycin (100 μg/ml)) for at least 30 d. The medium was changed every day. Two independent lines of monkey ES cells (CMK-6 and CMK-9) differentiated into retinal cells by this method.

Human ES cells. The human ES cells were used in accordance with the human ES cell research guidelines of the Japanese government. Two independent lines of human ES cells (khES-1 and khES-3) were maintained as previously described[43,44]. Briefly, undifferentiated human ES cells were maintained on a feeder layer of mitomycin C–treated mouse embryonic fibroblasts (Oriental Yeast). Human ES cells were maintained in DMEM/F-12 supplemented with 0.1 mM 2-mercaptoethanol, 0.1 mM nonessential amino acids, 2 mM L-glutamine, 20% KSR and 4 ng/ml bFGF (Upstate Biotechnology) in a humidified atmosphere of 2% CO_2 and 98% air at 37 °C. ES cells were passaged with 0.25% trypsin and 0.1 mg/ml collagenase IV (GIBCO) in PBS containing 1 mM $CaCl_2$ and 20% KSR every 3–4 d. For storage, the human ES colonies were suspended in ice-cold culture medium supplemented with 2M DMSO, 1M acetamide and 3M polypropylene glycol, and quickly frozen with liquid N2. The human ES cell lines expressed the undifferentiated ES cell markers Oct-3/4 and Nanog. These human ES cells were immunonegative for pan-neural markers such as nestin, βIII-tubulin and microtubule-associated protein-2(a+b), consistent with human ES cells remaining undifferentiated in our cultures.

For directed differentiation, ES colonies were partially dissociated into clumps (5–10 cells per clump) by treatment with 0.25% trypsin and 0.1 mg/ml collagenase IV in PBS containing 1 mM $CaCl_2$ and 20% KSR, followed by gentle trituration. Feeders were removed by incubation of the ES clumps on a gelatin-coated dish. ES clumps, at a density of 6.7 × 10^3 ES clumps/ml, were incubated in a nonadhesive bacterial-grade dish in DMEM/F-12 supplemented with 0.1 mM 2-mercaptoethanol, 0.1 mM nonessential amino acids, 2 mM L-glutamine, and 20% KSR for 2 d, in 20% KSR-containing ES differentiation medium (G-MEM, 0.1 mM nonessential amino acids, 1 mM pyruvate and 0.1 mM 2-mercaptoethanol) for 4 d, then in 15% KSR-containing ES differentiation medium for 8 d, and subsequently in 10% KSR-containing ES differentiation medium for 6 d. Dkk-1 (100 ng/ml) and Lefty-A (500 ng/ml) were applied to the medium for 20 d while in suspension culture. ES cell aggregates were then replated *en bloc* on poly-D-lysine/laminin/fibronectin-coated 8-well culture slides at a density of 10–15 aggregates per cm^2. In adherent cultures, cells were incubated in 10% KSR-containing ES differentiation medium.

For photoreceptor differentiation, human ES cells were incubated under SFEB/DL conditions for 90–120 d, and subsequently in RA/T medium [GMEM + 5% KSR + retinoic acid (1 μM) + taurine (100 μM) + N2 supplement + penicillin (100 units/ml)/streptomycin (100 μg/ml)] for at least 30 d. The medium was changed every day. Two independent lines of human ES cells (khES1 and khES3) differentiated into retinal cells by this method.

Immunocytochemistry. Cells were fixed with 4% paraformaldehyde and immunolabeled as described previously[13,44–46]. The primary antibodies and their working dilutions were as follows: mouse anti-BrdU (1:100, Roche), mouse anti-βIII-tubulin (1:500, Sigma), rabbit anti-blue opsin (1:500, Chemicon), rabbit anti-calbindin (1:200, Chemicon), rat anti-Crx (1:200), rabbit anti-active caspase-3 (1:500, BD Pharmingen), rabbit anti-cyclin D3 (1:200, Santa Cruz), mouse-anti-Islet1/2 (1:200, Developmental Studies Hybridoma Bank), mouse anti-Ki67 (1:200, BD Pharmingen), mouse anti-microtubule-associated protein-2(a+b) (1:500, Sigma), mouse anti-Mitf (1:30, Abcam), rabbit anti-Nanog (1:1000, ReproCELL), rabbit anti-nestin (1:1000, Covance), mouse anti-Oct3/4 (1:200, BD Pharmingen), rabbit anti-Pax6 (1:600, Covance), mouse anti-Pax6 (1:200, Developmental Studies Hybridoma Bank), mouse anti-Pax6 (1:500, R&D systems), rabbit anti-PCNA (1:100, Santa Cruz), rabbit anti-PKCα (1:1000, Sigma), rabbit anti-recoverin (1:3000, Chemicon), rabbit anti-red/green opsin (1:500, Chemicon), mouse anti-rhodopsin (RET-P1,

1:2000, Sigma), rabbit anti-RPE-65 (1:1000), rabbit anti-Rx (1:200), mouse anti-syntaxin (HPC-1, 1:2000, Sigma) and rabbit anti-ZO-1 (1:100, Zymed). Antibodies against Crx and Rx were obtained as previously described[12]. Polyclonal antiserum against RPE-65 was raised in rabbits immunized with the synthetic peptide CNFITKINPETLETIK and was used after purification. The secondary antibodies used were as follows: anti-mouse IgG, anti-rabbit IgG, and anti-rat IgG antibodies conjugated with Cy3 or FITC (1:300, Jackson Immunoresearch Laboratories). The immunoreactivity of each antibody was confirmed by immunostaining with appropriate retinal tissues as a positive control under the same conditions. F-actin was stained with Alexa Fluor 488-conjugated phalloidin (Molecular Probes). Cell nuclei were counterstained with 4′,6-diamidino-2-phenylindole (DAPI; 1 μg/ml, Molecular Probes) or TOTO-3 (Molecular Probes). Labeled cells were imaged with a laser-scanning confocal microscope (Leica) and apotome (Zeiss).

FACS analysis. SFEB/DLFA-treated ES cell aggregates were dissociated with trypsin (0.25%, Invitrogen) and DNase I (10 μg/ ml, Sigma) into single cells on day 9. After neutralization, the cells were resuspended in HBSS containing 0.1% BSA and 5 μg/ml propidium iodide (PI, Sigma), and passed through a cell strainer (BD), as described previously[17,47]. Cells were counted and sorted by FACS Aria (BD Biosciences), and the data were analyzed with FACS Diva software (BD Biosciences). Dead cells were excluded by gating forward and side scatter and by PI staining. Cells with Rx-GFP fluorescence (band pass filter: FITC, 530 nm) were sorted for further culture.

Reverse transcriptase-polymerase chain reaction (RT-PCR). Total RNA was extracted with RNeasy (QIAGEN), treated with RNase-free DNase I and reverse-transcribed with first-strand cDNA synthesis kit (Amersham Biosciences) as previously described[17,45]. The synthesized cDNA was amplified with gene-specific primers. The PCR products were separated by electrophoresis on a 2% agarose gel and detected under UV illumination. The primers used are available in **Supplementary Methods** online.

Electron microscopic analysis. Cells were fixed with 2% glutaraldehyde in 0.1 M PB for 10 min, postfixed with 1% osmium oxide in 0.1 M PB at pH 7.3, dehydrated by passage through a graded series of ethanol solutions (50%, 60%, 70%, 80%, 90%, 99.5% and 100%), and embedded in epoxy resin. From these samples, ultrathin sections were cut with an ultra-microtome, stained with 1% uranyl acetate and lead citrate, and then imaged with an electron microscope.

For a latex bead phagocytosis assay, cells were incubated in the medium containing Cy3-conjugated 1 μm polystyrene microspheres (Invitrogen) at a concentration of 1.0×10^8 beads/ml for 6 h at 37 °C. The cells were washed with culture medium, and then processed for transmission electron microscopy.

***Ex vivo* transplantation.** All animal procedures were approved by our institutional animal experimentation committee, and were in accordance with the ARVO Statement for the Use of Animals in Ophthalmic and Vision Research. Retinal explant cultures were prepared as described previously[13,45,48]. Briefly, neural retinal tissues from P8 mice (Nihon SLC) were excised and separated from other ocular tissues. The neural retina was placed onto a microporous membrane (30 mm in diameter; Millicell-CM, Millipore) with the ganglion cell layer facing up, and placed in a six-well culture plate. Each well contained 1 ml of culture medium consisting of 50% MEM/Hepes (Sigma), 25% HBSS, and 25% heat-inactivated horse serum (GIBCO) supplemented with 200 μM L-glutamine and 5.75 mg/ml glucose.

Mouse ES cells were treated with SFEB/DLFA, purified with FACS and treated with DAPT and retinoic acid/taurine/Shh/aFGF/bFGF. These cells were labeled with the FITC-labeling reagent (carboxyfluorescein diacetate succinimidyl ester, 7.5 μM; Molecular Probes) for 7 min on day 26, and dissociated with trypsin-EDTA and DNaseI into single cells. Two microliters of cell suspension (2×10^5 cells) were placed on the filter membrane before the retina was positioned on the membrane (subretinal space). The retina was maintained in a humidified atmosphere of 5% CO_2 and 95% air at 34 °C, with a change of culture medium every other day. For immunohistochemistry, the retinal explants were fixed and sectioned at 14-μm thick, as described previously[45,48]. Anti-FITC antibody was used to enhance detection.

Statistical analysis. Values are expressed as means ± s.e.m. At least 100–200 colonies and 2,500 cells were examined in each experiment. All sets of experiments were performed at least three times. Statistical analyses were performed with GraphPad Prism version 5.0 or InStat version 3.0 (GraphPad Software Inc.). The statistical significance of difference was determined by ANOVA followed by Tukey's test (**Figs. 1f**, **3g** and **Supplementary Fig. 3c** online) or Dunnett's test (**Figs. 3b** and **4b**), and by two-way ANOVA followed by Bonferroni test (**Fig. 2a** and **Supplementary Fig. 4d–f** online). Data from **Figure 5a,d,e,h,i** were evaluated by an unpaired *t*-test. Probability values $<5\%$ were considered significant.

Note: Supplementary information is available on the Nature Biotechnology website.

ACKNOWLEDGMENTS

We thank J. Takahashi (Kyoto University, Kyoto, Japan) for providing the monkey ES cell line, H. Suemori and N. Nakatsuji (Kyoto University) for providing the human ES cell line, S. Nakagawa (RIKEN, Japan), T. Kume, H. Katsuki (Kyoto University), M. Haruta and M. Akimoto (Kyoto University Hospital) for valuable comments on this work, S. Nishikawa, M. Osawa and T. Era (RIKEN) for advice on FACS, K. Iseki and S. Yonemura (Riken) for the electron microscopic analysis, T. Yokota, A. Nomori, N. Ishibashi and A. Nishiyama for excellent technical assistance, and members of the Takahashi laboratory, the Sasai laboratory and the Akaike laboratory for discussions. This work was supported by Grants-in-Aid from the Ministry of Education, Culture, Sports, Science and Technology, and the Leading Project (M.T. and Y.S.). This study was also supported by Grants-in-Aid for Scientific Research from the Japan Society for the Promotion of Science, and the Mochida Memorial Foundation for Medical and Pharmaceutical Research (F.O.).

AUTHOR CONTRIBUTIONS

F.O. designed research, performed experiments, wrote the paper and provided financial support. H.I. designed research, performed experiments and wrote the paper. M.M., T.W. and K.W. performed experiments. N.Y., A.A. and Y.S. coordinated the project. M.T. provided financial support and supervised the whole project. All authors discussed the results and commented on the manuscript.

Published online at http://www.nature.com/naturebiotechnology/
Reprints and permissions information is available online at http://npg.nature.com/reprintsandpermissions

1. Rattner, A. & Nathans, J. Macular degeneration: recent advances and therapeutic opportunities. *Nat. Rev. Neurosci.* **7**, 860–872 (2006).
2. Kaplan, H.J., Tezel, T.H., Berger, A.S., Wolf, M.L. & Del Priore, L.V. Human photoreceptor transplantation in retinitis pigmentosa. A safety study. *Arch. Ophthalmol.* **115**, 1168–1172 (1997).
3. Takahashi, M., Palmer, T.D., Takahashi, J. & Gage, F.H. Widespread integration and survival of adult-derived neural progenitor cells in the developing optic retina. *Mol. Cell. Neurosci.* **12**, 340–348 (1998).
4. Aramant, R.B., Seiler, M.J. & Ball, S.L. Successful cotransplantation of intact sheets of fetal retina with retinal pigment epithelium. *Invest. Ophthalmol. Vis. Sci.* **40**, 1557–1564 (1999).
5. Radtke, N.D., Aramant, R.B., Seiler, M.J., Petry, H.M. & Pidwell, D. Vision change after sheet transplant of fetal retina with retinal pigment epithelium to a patient with retinitis pigmentosa. *Arch. Ophthalmol.* **122**, 1159–1165 (2004).
6. MacLaren, R.E. *et al.* Retinal repair by transplantation of photoreceptor precursors. *Nature* **444**, 203–207 (2006).
7. Haruta, M. *et al.* In vitro and in vivo characterization of pigment epithelial cells differentiated from primate embryonic stem cells. *Invest. Ophthalmol. Vis. Sci.* **45**, 1020–1025 (2004).
8. Haruta, M. *et al.* Induction of photoreceptor-specific phenotypes in adult mammalian iris tissue. *Nat. Neurosci.* **4**, 1163–1164 (2001).
9. Sun, G. *et al.* Retinal stem/progenitor properties of iris pigment epithelial cells. *Dev. Biol.* **289**, 243–252 (2006).
10. Tropepe, V. *et al.* Retinal stem cells in the adult mammalian eye. *Science* **287**, 2032–2036 (2000).
11. Zhao, X., Liu, J. & Ahmad, I. Differentiation of embryonic stem cells into retinal neurons. *Biochem. Biophys. Res. Commun.* **297**, 177–184 (2002).
12. Hirano, M. *et al.* Generation of structures formed by lens and retinal cells differentiating from embryonic stem cells. *Dev. Dyn.* **228**, 664–671 (2003).
13. Ikeda, H. *et al.* Generation of $Rx^+/Pax6^+$ neural retinal precursors from embryonic stem cells. *Proc. Natl. Acad. Sci. USA* **102**, 11331–11336 (2005).
14. Lamba, D.A., Karl, M.O., Ware, C.B. & Reh, T.A. Efficient generation of retinal progenitor cells from human embryonic stem cells. *Proc. Natl. Acad. Sci. USA* **103**, 12769–12774 (2006).
15. Thomson, J.A. *et al.* Embryonic stem cell lines derived from human blastocysts. *Science* **282**, 1145–1147 (1998).

16. Hoffman, L.M. & Carpenter, M.K. Characterization and culture of human embryonic stem cells. *Nat. Biotechnol.* **23**, 699–708 (2005).
17. Watanabe, K. *et al.* Directed differentiation of telencephalic precursors from embryonic stem cells. *Nat. Neurosci.* **8**, 288–296 (2005).
18. Mathers, P.H., Grinberg, A., Mahon, K.A. & Jamrich, M. The *Rx* homeobox gene is essential for vertebrate eye development. *Nature* **387**, 603–607 (1997).
19. Furukawa, T., Kozak, C.A. & Cepko, C.L. *rax*, a novel paired-type homeobox gene, shows expression in the anterior neural fold and developing retina. *Proc. Natl. Acad. Sci. USA* **94**, 3088–3093 (1997).
20. Furukawa, T., Morrow, E.M. & Cepko, C.L. *Crx*, a novel *otx*-like homeobox gene, shows photoreceptor-specific expression and regulates photoreceptor differentiation. *Cell* **91**, 531–541 (1997).
21. Chen, S. *et al.* Crx, a novel Otx-like paired-homeodomain protein, binds to and transactivates photoreceptor cell-specific genes. *Neuron* **19**, 1017–1030 (1997).
22. Kubo, F., Takeichi, M. & Nakagawa, S. Wnt2b inhibits differentiation of retinal progenitor cells in the absence of Notch activity by downregulating the expression of proneural genes. *Development* **132**, 2759–2770 (2005).
23. Jadhav, A.P., Mason, H.A. & Cepko, C.L. Notch 1 inhibits photoreceptor production in the developing mammalian retina. *Development* **133**, 913–923 (2006).
24. Yaron, O. *et al.* Notch1 functions to suppress cone-photoreceptor fate specification in the developing mouse retina. *Development* **133**, 1367–1378 (2006).
25. Dovey, H.F. *et al.* Functional gamma-secretase inhibitors reduce beta-amyloid peptide levels in brain. *J. Neurochem.* **76**, 173–181 (2001).
26. Geling, A. *et al.* A γ-secretase inhibitor blocks Notch signaling in vivo and causes a severe neurogenic phenotype in zebrafish. *EMBO Rep.* **3**, 688–694 (2002).
27. Levine, E.M., Fuhrmann, S. & Reh, T.A. Soluble factors and the development of rod photoreceptors. *Cell. Mol. Life Sci.* **57**, 224–234 (2000).
28. Altshuler, D. & Cepko, C. A temporally regulated, diffusible activity is required for rod photoreceptor development in vitro. *Development* **114**, 947–957 (1992).
29. Young, T.L. & Cepko, C.L. A role for ligand-gated ion channels in rod photoreceptor development. *Neuron* **41**, 867–879 (2004).
30. Hyatt, G.A. & Dowling, J.E. Retinoic acid. A key molecule for eye and photoreceptor development. *Invest. Ophthalmol. Vis. Sci.* **38**, 1471–1475 (1997).
31. McGinnis, J.F. *et al.* Unique retina cell phenotypes revealed by immunological analysis of recoverin expression in rat retina cells. *J. Neurosci. Res.* **55**, 252–260 (1999).
32. Lukats, A. *et al.* Photopigment coexpression in mammals: comparative and developmental aspects. *Histol. Histopathol.* **20**, 551–574 (2005).
33. Bora, N., Conway, S.J., Liang, H. & Smith, S.B. Transient overexpression of the Microphthalmia gene in the eyes of Microphthalmia vitiligo mutant mice. *Dev. Dyn.* **213**, 283–292 (1998).
34. Nguyen, M. & Arnheiter, H. Signaling and transcriptional regulation in early mammalian eye development: a link between FGF and MITF. *Development* **127**, 3581–3591 (2000).
35. Baumer, N. *et al.* Retinal pigmented epithelium determination requires the redundant activities of Pax2 and Pax6. *Development* **130**, 2903–2915 (2003).
36. Burke, J.M. Determinants of retinal pigment epithelial cell phenotype and polarity. in *The Retinal Pigment Epithelium* (eds. Marmor, M.F. & Wolfensberger, T.J.) 86–102 (Oxford Univ. Press, New York, 1998).
37. Boulton, M. Melanin and the retinal pigment epithelium. in *The Retinal Pigment Epithelium* (eds. Marmor, M.F. & Wolfensberger, T.J.) 68–85 (Oxford Univ. Press, New York, 1998).
38. Martin, M.J., Muotri, A., Gage, F. & Varki, A. Human embryonic stem cells express an immunogenic nonhuman sialic acid. *Nat. Med.* **11**, 228–232 (2005).
39. Takahashi, K. *et al.* Induction of pluripotent stem cells from adult human fibroblasts by defined factors. *Cell* **131**, 861–872 (2007).
40. Pouton, C.W. & Haynes, J.M. Embryonic stem cells as a source of models for drug discovery. *Nat. Rev. Drug Discov.* **8**, 605–616 (2007).
41. Suemori, H. *et al.* Establishment of embryonic stem cell lines from cynomolgus monkey blastocysts produced by IVF or ICSI. *Dev. Dyn.* **222**, 273–279 (2001).
42. Kawasaki, H. *et al.* Generation of dopaminergic neurons and pigmented epithelia from primate ES cells by stromal cell-derived inducing activity. *Proc. Natl. Acad. Sci. USA* **99**, 1580–1585 (2002).
43. Suemori, H. *et al.* Efficient establishment of human embryonic stem cell lines and long-term maintenance with stable karyotype by enzymatic bulk passage. *Biochem. Biophys. Res. Commun.* **345**, 926–932 (2006).
44. Ueno, M. *et al.* Neural conversion of ES cells by an inductive activity on human amniotic membrane matrix. *Proc. Natl. Acad. Sci. USA* **103**, 9554–9559 (2006).
45. Osakada, F. *et al.* Wnt signaling promotes regeneration in the retina of adult mammals. *J. Neurosci.* **27**, 4210–4219 (2007).
46. Mizuseki, K. *et al.* Generation of neural crest-derived peripheral neurons and floor plate cells from mouse and primate embryonic stem cells. *Proc. Natl. Acad. Sci. USA* **100**, 5828–5833 (2003).
47. Su, H.L. *et al.* Generation of cerebellar neuron precursors from embryonic stem cells. *Dev. Biol.* **290**, 287–296 (2006).
48. Suzuki, T. *et al.* Chondroitinase ABC treatment enhances synaptogenesis between transplant and host neurons in model of retinal degeneration. *Cell Transplant.* **16**, 493–503 (2007).